Studies on underlying mechanism of interlimb coordination of legged robots using nonlinear oscillators

Soichiro Fujiki

Acknowledgement

First and foremost, I would like to express my sincere gratitude to Dr. Kei Senda, Professor of Department of Aeronautics and Astronautics, Graduate School of Engineering, Kyoto University, for his continuous guidance and support. Without his valuable advice and comments, this thesis would never be completed.

I would like to express appreciation to Dr. Kenji Fujimoto, Professor of Department of Aeronautics and Astronautics, Graduate School of Engineering, Kyoto University, and Dr. Fumitoshi Matsuno, Professor of Mechanical Engineering and Science, Graduate School of Engineering, Kyoto University, for their valuable comments and suggestions.

I would like to extend the deepest appreciation to Dr. Shinya Aoi, Lecturer of Department of Aeronautics and Astronautics, Graduate School of Engineering, Kyoto University, for his continuous guidance and grateful support thorough out my research. He has tirelessly used exertion for teaching and supporting me. Without his valuable advice and support, this thesis would not have materialized.

I would like to express my cordial gratitude to Dr. Tsuchiya Kazuo, Professor of Department of Aeronautics and Astronautics, Graduate School of Engineering, Kyoto University, for his invaluable comments and suggestions. I was indeed stimulated by discussion with him and strongly influenced by his perspective to researches.

I would like to express appreciation to Dr. Tetsuro Funato, Assistant Professor of Department of Mechanical Engineering and Intelligent Systems, Graduate School of Informatics and Engineering, The University of Electro-Communications, and Dr. Nozomi Tomita, Research associate of Department of Mathematics, Graduate School of Science, Kyoto University, for the collaboration in experimental works and their useful comments and discussions.

I would like to express appreciation to Dr. Dai Yanagihara, Associate Professor of Department of Life Sciences, Graduate School of Arts and Sciences, The University of Tokyo, for the collaboration in experimental work. I was taught a lot of things through the experiment with him.

I would like to express appreciation to Dr. Naoto Yokoyama, Assistant Professor of Department of Aeronautics and Astronautics, Graduate School of Engineering, Kyoto University, for his encouragement and advice. I got refreshed by taking a coffee break with him and he sometimes gave me advices to solve my minor technical problems.

I would like to thank the members of the laboratory of Dynamics in Aeronautics and Astronautics and the laboratory of Systems and Control. Thanks to seminar, discussion, experiment, conversation, and activity with them, I have fully enjoyed my student life. Especially, I would like to express appreciation to Mr. Tsuyoshi Yamashita. By the virtue of his comprehensible explanations, I could obtain the technique to perform the robot experiment.

Lastly, I am deeply grateful to my parents, Hirokazu and Chie Fujiki, for their generous attitude, constant support, and warm encouragement during my student life.

Contents

Chapter 1

Introduction

1.1 Background

To explore planets and satellites, such as moon and mars, various robots have been used. Because it takes much time for the robots to receive a command from the earth, the robots are required to be highly autonomous. Furthermore, planets and satellites have various terrains, such as craters, rocks, sand, and slopes, and the robots have to be highly robust and adaptive to complete a task in such environments.

So far, many legged robots have been developed to establish high robustness and adaptability in diverse environments [17, 38, 77, 78, 115, 116]. Because the legged robots generally have some legs and each leg consists of some links and joints, the robots have a large number of degrees of freedom. Although such a large number of degree-of-freedom contributes to variety of movements, it is difficult to plan and control the robot movements.

Humans and animals also have many joints. Although they have a large number of degree-of-freedom, they create adaptive locomotion by producing proper relationship of the movements between the legs. Such coordinative movements between the legs are called interlimb coordination. The most typical example of interlimb coordination is gait. Quadruped animals use various gait, such as walk, crawl, trot, pace, gallop, and

bounce [11]. Insects use metachronal and tripod gaits. Such gaits are characterized by the relative phase between the movements of the legs, which shows the change in the interlimb coordination. Their gaits change depending on the locomotion speed. In a low speed range, the quadruped animals show walk and crawl. In a middle speed range, they show trot and pace. In a high speed range, they show gallop and bounce. As to insects, they show metachronal gait in a low speed range and tripod gait in a high speed range. Researches suggested that the reason why they change the gaits depending on the locomotion speed is to reduce the energy consumption [49, 58] or to reduce the load on their legs [36]. However, underlying mechanism remains unclear. It is expected that if the underlying mechanism in producing interlimb coordination of humans and animals is revealed, the mechanism is useful to design a control system of legged robots. For this purpose, understanding the functional roles of the nervous system for the interlimb coordination is necessary.

The structure and functional roles of the central nervous system, which controls the musculoskeletal system of human and animals, are so complicated that they have not been fully clarified. However, from neurophysiological findings, animals have a neural circuit called central pattern generator (CPG), which produce rhythmic motor commands [50, 53]. The CPG strongly contributes to generating rhythmic motions, such as walking, swimming, and flying by producing rhythm and phase and sending motor commands to muscles. It has a crucial role in the interlimb coordination. Both invertebrate and vertebrate have such a neural circuit [51, 81]. The nervous system in an insect, which is invertebrate, has a structure called ladder-like nervous system. Two long nervous traverse longitudinally through the body from the head to back side and there are clusters of neuron nearby the organ of senses and motor organ. These clusters connect the two long nervous. It is reported that the neurons controlling the flight muscle in locus [124] and clustered neurons nearby the leg in stick insect [12] showed the rhythmic neural activity. In vertebrate, such as quadruped animals, the CPG exists in the spinal cord. Spinal cat walked on treadmill changed the gait from walk to trot and from trot to gallop by increasing the speed of the treadmill [40]. This suggests that the spinal cord contributes to producing gaits and gait transition. To change the interlimb coordination,

sensory information plays an important role. In particular, the CPG resets the producing rhythm and shifts the phase [25, 42, 117]. The generation of rhythmic motor commands and modulation of the commands based on sensory afferent in the CPG are the lowest level sensorimotor function.

In addition to the spinal cord, the cerebellum in vertebrate also contributes to modulating the motor commands [13, 64]. The Purkinje cells in the cerebellum show synaptic plasticity (long term depression) [64]. It is suggested that such synaptic plasticity in the cerebellum contributes to the motor learning. Lack of this plasticity prevents from obtaining a new gait through learning [135]. Such a feature has been seen in splitbelt treadmill walking of humans and animals. This treadmill has two parallel belts and each belt speed is controlled independently. It can produce symmetric (tied configuration) and asymmetric (splitbelt configuration) environments [86, 111]. Healthy people show two types of adaptations. When the speed condition changes from the tied to splitbelt configuration, interlimb coordination rapidly changes (early adaptation). By continuing the walking on the condition, it gradually changes to return to the state in the tied configuration (late adaptation). It is reported that spinal cats showed the early adaptation in interlimb coordination [40, 42] and people with cerebellar damage did not show late adaptation in interlimb coordination [88]. However, it remains unclear how neural systems contribute to the interlimb coordination.

1.2 Approach

To investigate the mechanism of generating adaptive locomotor behavior, neurophysiological studies have investigated the nervous systems. In the early 20th century, by observing the reciprocal activations of the flexor and extensor of cat's hindlimb during locomotion, Brown [18] proposed a concept "half-center" as a nervous system model controlling such activities of muscles. He suggested that the neurons controlling flexor and extensor inhibited each other and this mutual inhibition produced the periodic and reciprocal activations of these muscles. Jankowska and Lundberg [68] reported that the existence of the interneurons, which have the structure corresponding to the half-center

model, could not be doubted according to their experiments.

However, it is difficult to fully understand essential function of the nervous system only by measuring neural activities. To overcome the limitation, physiological model to reconstruct the measured data is useful. Matsuoka [82, 83] focused on the feature of a neuron and he showed that two elements inhibiting each other generate periodic behavior by his mathematical model. This Matsuoka oscillator has been used for control system of legged robots [63, 73, 125]. However, because the Matsuoka oscillator model was proposed to reconstruct the rhythmic pattern of the mutually inhibiting neurons, we have to determine large amounts of control parameters and it is difficult to use for locomotion control system. Assuming limit cycles and using phase reduction theorem, we can explain periodic neural activations by an easier form [22, 75]. Based on this, recent studies often used a simple oscillator model [61, 101]. Ryback *et al.* [113, 114] focused on the issue that there were phenomena observed in many physiological experiments about locomotion, which cannot be explained by the earlier half center model. They improved the half center model and proposed a model with hierarchical two layers of interneurons. Aoi and Tsuchiya [7] showed that by using nonlinear oscillators, which have two-layered structure, a biped robot walked adaptively when the slope of the floor changed and the robot was disturbed by external force.

So far, many researchers have studied about modeling the CPG and controlling locomotion. In this thesis, we focused on the mechanism of interlimb coordination. Locomotion is generated through the dynamic interaction between the nervous system, body mechanical system, and the environment. Therefore, we have to consider integrated systems of these three elements. Instead of investigating the neural activity in biological system, we used simple models of these three elements and investigated the generated behavior from a dynamic viewpoint. In particular, we used legged robots for the body mechanical system and nonlinear oscillators for the control system.

1.3 Outline of this thesis

As mentioned above, the most basic example in interlimb coordination is animal gait. Animals show many gaits and change them when they change the locomotion speed. In addition, the hysteresis appears in their gait transitions, which is a typical characteristic in nonlinear dynamics. However, it remains unclear why such a phenomenon occurs. As the experiment of treadmill walking of spinal cats suggested, gait transition can be induced by rhythmic motor commands and modulation of the commands based on sensory afferent in the CPG. In this thesis, in Chapter 2, we developed a locomotion control system of a hexapod robot using nonlinear oscillator based on CPG, and investigated gait transition of a hexapod robot by changing locomotion speed through computer simulation. In particular, we focused on the hysteresis property in the gait transition. Through this simulation experiment, we verify if our nervous control system using oscillators captures the function of the actual nervous system about interlimb coordination in animals from a dynamic viewpoint.

As mentioned above, spinal cats changed interlimb coordination in splitbelt treadmill walking. This suggests that the spinal code contributes to the interlimb coordination (in this case, it is called early adaptation). In Chapter 3, we used the locomotion system developed in Chapter 2, and investigated the interlimb coordination of a biped robot walking on a splitbelt treadmill. We examined if early adaptation in the interlimb coordination appears similarly to humans. In addition to the spinal cord, in Chapter4, we focused on the cerebellum, which contributes to motor learning. We incorporated a learning model to the spinal model in Chapter 3 and examined if the robot shows late adaptation in the interlimb coordination similarly to humans.

Specifically, these chapters are organized as follows: In Chapter 2, we used a hexapod robot for the body mechanical system, oscillator network model, which consists of six phase oscillators with phase resetting, for the nervous system, and flat ground for the environment. The gait is determined by the relative phases between the oscillators, which is five degree-of-freedom. Based on the feature of insect's gait as Wilson pointed out [132], we used constraint conditions to the oscillator phases, which reduced degree-of-freedom

from five to one. Using computer simulation, we examined if our model changed its gait by changing the locomotion speed and hysteresis emerged in gait transition. We investigated stability structure of the gait using a first return map.

In Chapter 3, we focused on the adaptive locomotor behavior in splitbelt treadmill walking induced by the spinal CPG (i.e. the early adaptation). We used a biped robot for the body mechanical system, oscillator network model for nervous system, and splitbelt treadmill for the environment. The two phase oscillators driving the leg motions have phase resetting mechanism. We performed the robot experiment to examine if without changing the control parameters, the robot showed the adaptive behavior when the speed condition of the treadmill changed from the tied to splitbelt configuration. We focused on the changes of locomotion parameters such as relative phase between the leg and duty factor of each leg (this is the ratio of the stance phase duration relative to one gait cycle duration) because these parameters remarkably change in human splitbelt treadmill walking. Furthermore, the changing trend of locomotion parameters of our robot was compared with measured human splitbelt treadmill walking. We clarify the adaptation mechanism from a dynamic viewpoint.

In Chapter 4, we also investigated a biped robot walking on a splitbelt treadmill, as in Chapter 3. In this chapter, we focused on motor learning in the cerebellum. Based on the function of the cerebellum, we developed a evaluation function about the error information between the predicted and actual foot contact timings and incorporated learning model to the locomotion control system of Chapter 3. We performed computer simulation and robot experiment to examine if the robot showed not only early adaptation but also late adaptation in the interlimb coordination. We investigated the changes in the relative phase between the legs, the duty factors, and the profile of center of pressure at the early and late stage of splitbelt configuration. These results were evaluated by measuring human splitbelt treadmill walking. In addition, we clarify the adaptation mechanism from a dynamic viewpoint.

At last in chapter 5, this thesis concluded and future works are pointed out.

Chapter 2

Gait generation and transition of a hexapod robot depending on locomotion speed

2.1 Introduction

Biological systems have various gaits in their locomotion and the gaits are characterized by the number of legs used for locomotion. Humans walk bipedally and use walking and running gaits in accordance with the locomotion speed. Quadrupeds have four legs and employ various gaits such as walking, trotting, and galloping. Insects (hexapods) with six legs use metachronal (wave) and tripod gaits. These gaits are characteristic locomotion patterns that are generated over a limited range of locomotion speeds, and they are described by parameters that vary discontinuously at the transition [11]. In thewalk-run transition of humans, the relative phase between the leg segments [that is, the intralimb (or intersegmental) coordination pattern] varies [31]. In contrast, in the walk-trot-gallop transition of quadrupeds and the metachronal-tripod gait transition of insects, the relative phase between the legs (i.e., the interlimb coordination pattern) changes [11, 132].

Locomotion is a self-organizing phenomenon that emerges through dynamic interactions among the nervous system, the musculoskeletal system, and the environment and

it has a number of nonlinear characteristics. In particular, hysteresis appears when the gaits change in accordance with the locomotion speed [3, 31, 49, 55, 60, 76, 109, 118, 128]. Specifically, the gaits vary at different locomotion speeds depending on the direction of speed change. Although hysteresis is a typical characteristic of nonlinear dynamic systems, the hysteresis mechanism in the gait transition of biological systems remains largely unclear.

So far, to elucidate the locomotor mechanisms in biological systems, biomechanical and physiological studies have been independently conducted. Biomechanical studies generally focus on the functional roles of the musculoskeletal system, whereas physiological studies mainly examine the configurations and activities of the neural system. However, locomotion is a well-organized motion generated through the body and the nervous system, and it is thus difficult to fully elucidate the locomotor mechanisms from a single perspective. To overcome the limitations of studies based on a single approach, neuromechanical models for the locomotion of biological systems have been developed by integrating the biomechanical and physiological findings [9, 27, 34, 59, 74, 96, 97, 103, 107, 125, 127, 130].

From the observation of locomotion, hysteresis has been reported in thewalk-run transition of humans [31, 60, 76, 109, 118, 128] and in the gait transitions of quadrupeds [3, 49, 55]. Neuromechanical models of humans and quadrupeds have been employed to investigate their gait transition mechanisms and have demonstrated that hysteresis appears in the walk-run transition of humans [125] and in the walk-trot transition of quadrupeds [9]. However, regarding insect locomotion, although the gaits of insects have been investigated [14, 29, 47, 70, 102, 132], to the best of our knowledge it remains unclear if hysteresis appears in the gait transitions of insects.

To date, oscillator network models have been used to examine the gait transition in insect locomotion [24, 47, 52, 72]. However, these models did not incorporate the contribution of the body mechanical system. In contrast, neuromechanical models for insect locomotion have been developed and help the understanding of the contributions of sensory-motor coordination to the generation of locomotion [34, 59, 74, 87, 107, 127, 130], but they did not investigate the gait transition mechanism. The aim of this study

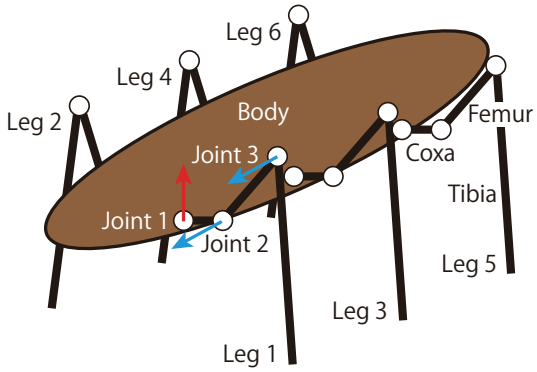

Fig. 2.1: Hexapod robot consisting of a body and six legs.

is to construct a neuromechanical model of an insect and to investigate the dynamic characteristics of its gait and gait transition. Specifically, we investigate what gaits our model produces depending on the locomotion speed and if the gaits vary when the locomotion speed is changed. Furthermore, we examine whether the gait transitions exhibit hysteresis and what dynamic structures produce the gait transitions.

2.2 Method

2.2.1 Haxapod robot

Figure 2.1 shows the hexapod robot, which consists of one rigid body and three pairs of legs (legs 1-6). Each leg has three rigid links (coxa, femur, and tibia). The body-coxa, coxa-femur, and femur-tibia joints are enumerated as joints 1, 2, and 3, respectively. Joint 1 moves the leg tip forward or backward relative to the body, and joints 2 and 3 raise or lower the leg tip. Leg joint movements are generated by motor commands from the nervous system model (see Sec. 2.2.2). We derived the equation of motion of this hexapod robot using a Lagrangian equation as in [9], where we used viscoelastic elements to model the contact between the leg tips and the ground and used large values for the viscoelastic parameters so that the leg tips rarely slipped during foot contact. We performed forward dynamic simulations by solving the equation of motion using a fourth-order Runge-Kutta method with a step size of 0.02 ms. Table 2.1 shows the physical parameters of the robot;

Table 2.1: Physical parameters of the hexapod robot.

Link	Parameter	Value
Body	Mass [g]	3.00
	Length [cm]	4.2
	Width [cm]	1.0
Coxa	Mass [g]	0.05
	Length [cm]	0.02
Femur	Mass [g]	0.03
	Length [cm]	0.2
Tibia	Mass [g]	0.03
	Length [cm]	1.0

the six legs had the same parameter values as each other.

2.2.2 Nervous system model

Physiological studies have shown that central pattern generators (CPGs) greatly contribute to producing motor commands for rhythmic leg movements in both vertebrates and invertebrates [12, 51, 81, 99, 119], which are located in the spinal cord of vertebrates and in the thoracic ganglia of invertebrates. Although the organization of CPGs remains unclear, physiological findings suggest that CPGs consist of hierarchical networks composed of rhythm generator (RG) and pattern formation (PF) networks [19, 71, 113]. The RG network produces the basic rhythm and the PF network shapes the rhythm into spatiotemporal patterns of motor commands. In this study, we modified the oscillator network model, which is a simple two-layer network system composed of RG and PF models and which is constructed for quadruped locomotion [9], to apply it for the nervous system model of an insect (Fig. 2.2).

Rhythm generator model

The RG model produces rhythm information for locomotion through dynamic interactions among the body mechanical system, the nervous system, and the environment. For the RG model, we used six simple phase oscillators (oscillators 1-6) to generate the basic

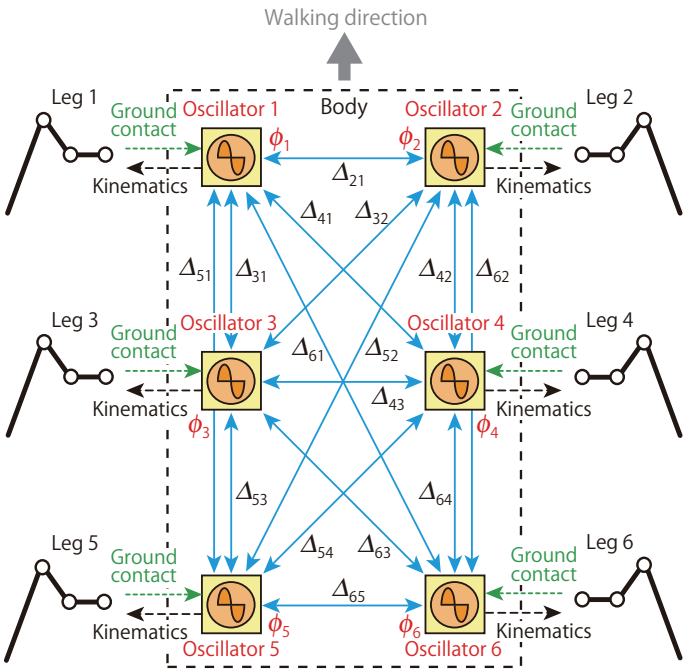

Fig. 2.2: Nervous system model using six oscillators. Solid blue arrows indicate interactions among the oscillators based on the phase relationship Δ_{ij}. The oscillator phases are modulated by tactile sensor information (dotted green arrows). The oscillator phases determine the leg joint kinematics.

rhythm and phase information for the corresponding leg based on commands related to the desired locomotion speed and gait. We denote the phase of the oscillator i ($i = 1, ..., 6$) by ϕ_i ($0 \leq \phi_i < 2\pi$) and used the following phase dynamics:

$$\dot{\phi}_i = \omega + g_{1i} + g_{2i}, \qquad i = 1, ..., 6 \tag{2.2.1}$$

where ω is the basic oscillator frequency (it has the same value for all six oscillators), g_{1i} is the interaction between the oscillators based on the interlimb coordination, and g_{1i} is the sensory regulation based on a phase resetting mechanism. The details of g_{1i} and g_{2i} are explained later in this section.

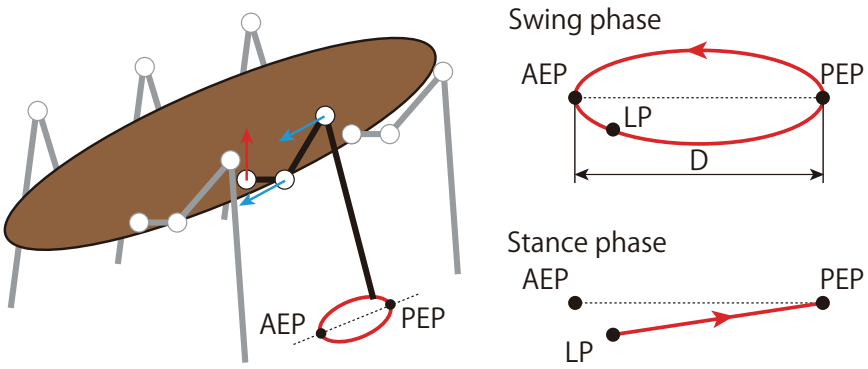

Fig. 2.3: Leg joint kinematics composed of swing and stance phases. The swing phase for the leg tip is a closed curve that includes the anterior extreme position (AEP) and the posterior extreme position (PEP). The stance phase is a straight line from the landing position (LP) to the PEP. When the leg lands on the ground, it changes from the swing to the stance phase.When the leg tip reaches the PEP, it moves into the swing phase.

Pattern formation model

Physiological studies have revealed that nervous systems receive sensory information and encode global parameters of the leg kinematics, such as the length and orientation of the limb axis (position of the leg tip relative to the root) [15, 20, 105]. We used the PF model to determine the leg kinematics based on the oscillator phase ϕ_i from the RG model and to produce motor torques for generating the desired kinematics.

Locomotion involves propelling the center of mass forward, which is achieved by moving the swing leg forward and by supporting the body and producing a propulsive force from the ground using the stance leg. We used a simple leg kinematics composed of the swing and stance phases (Fig. 2.3). The swing phase consists of a simple closed curve for the leg tip that includes the anterior extreme position (AEP) and the posterior extreme position (PEP). It starts from the PEP and continues until the leg touches the ground. The line segment between the AEP and the PEP is parallel to the body. The stance phase is a straight line from the landing position (LP) to the PEP. During this phase, the leg tip moves in the opposite walking direction relative to the body. The body travels in the walking direction while the leg tips are in contact with the ground.

We used D for the distance between the AEP and the PEP. We denote the swing and

stance phase durations by $T_{\rm sw}$ and $T_{\rm st}$, respectively, for the casewhen the leg tip contacts the ground at the AEP (LP = AEP). The duty factor β (the ratio between the stance phase and the step cycle duration), the basic frequency ω in (2.2.1), the locomotion speed v, and the stride length S are, respectively, given by

$$\begin{aligned} \beta &= \frac{T_{\rm st}}{T_{\rm sw}+T_{\rm st}} \\ \omega &= \frac{2\pi}{T_{\rm sw}+T_{\rm st}} \\ v &= \frac{D}{T_{\rm st}} \\ S &= \frac{D}{\beta} \end{aligned} \tag{2.2.2}$$

We used $D = 2$ mm and $T_{\rm sw} = 34$ ms and varied v by changing β through $T_{\rm st}$ in the samemanner as observed in the locomotion of biological systems [29, 30, 57, 99, 102], where ω and S also varied with β. We used the same values of these parameters for all the legs.

These trajectories for the swing and stance phases are given as functions of the corresponding oscillator phase, where we used $\phi_i = 0$ at the PEP and $\phi_i = \phi_{\rm AEP}$ $[= 2\pi(1-\beta)]$ at the AEP. Therefore, the desired joint kinematics is given as a function of the oscillator phase and each joint is controlled by the joint torque based on proportional-derivative (PD) feedback control to produce the desired kinematics.

Gait pattern

Because the leg kinematics is determined by the corresponding oscillator phase, the interlimb coordination pattern is determined by the relative phase between the oscillators. We denote the relative phase by the matrix $\Delta_{ij} = \phi_i - \phi_j$ $(i, j = 1, ..., 6,\ 0 \leq \Delta_{ij} < 2\pi)$. As the relationships $\Delta_{ij} = -\Delta_{ji}$, $\Delta_{ij} = \Delta_{ik} + \Delta_{kj}$, and $\Delta_{ii} = 0$ $(i, j, k = 1, ..., 6)$ are satisfied, the gait is determined by five state variables, such as $[\Delta_{21}\ \Delta_{31}\ \Delta_{43}\ \Delta_{53}\ \Delta_{65}]$. For example, $[\Delta_{21}\ \Delta_{31}\ \Delta_{43}\ \Delta_{53}\ \Delta_{65}] = [\pi\ 2\pi/3\ \pi\ 2\pi/3\ \pi]$ is satisfied for the metachronal gait and $[\Delta_{21}\ \Delta_{31}\ \Delta_{43}\ \Delta_{53}\ \Delta_{65}] = [\pi\ \pi\ \pi\ \pi\ \pi]$ is satisfied for the tripod gait (Fig. 2.4).

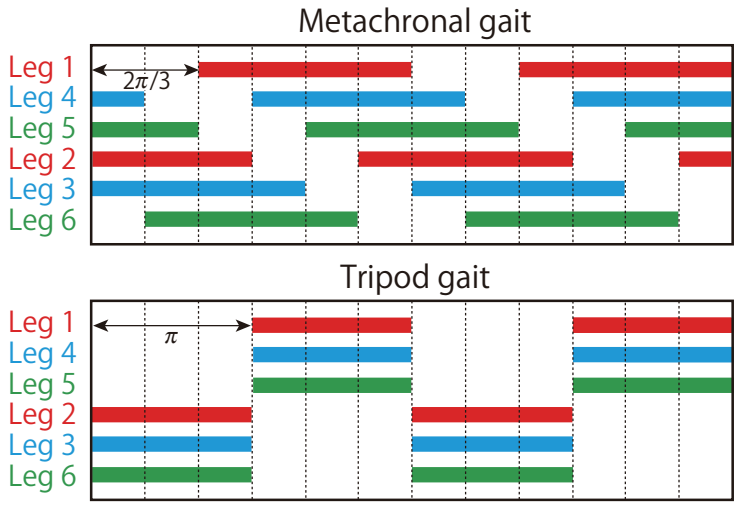

Fig. 2.4: Footprint diagrams for metachronal and tripod gaits, where the right and left legs move in antiphase [red, fore legs (legs 1 and 2); blue, middle legs (legs 3 and 4); green, hind legs (legs 5 and 6)].

Function g_{1i} in (2.2.1) manipulates these relative phases, which is given by

$$g_{1i} = -\sum_{j=1}^{6} K_{ij}\sin(\Delta_{\mathrm{ij}} - \Delta^*_{\mathrm{ij}}), \quad \mathrm{i} = 1, ..., 6 \tag{2.2.3}$$

where Δ^*_{ij} $(i, j = 1, ..., 6)$ is the desired relative phase and K_{ij} $(i, j = 1, ..., 6)$ is the gain constant $(K_{ij} \geq 0)$. When a large value is used for K_{ij}, the relationship $\Delta_{ij} = \Delta^*_{ij}$ is satisfied. The solid blue arrows in Fig. 2.2 indicate these interactions among the oscillators.

Phase resetting

To produce adaptive and effective locomotor behaviors, adequate sensory regulation of motor commands is crucial. Physiological studies have shown that the locomotor rhythm and phase are modulated by producing phase shift and rhythm resetting based on sensory afferents and perturbations (phase resetting) [12, 25, 32, 113, 117]. In addition, neuromusculoskeletal models have demonstrated the contributions of phase resetting to the generation of adaptive locomotion [4, 5, 95, 134].

In this study, we incorporated the phase resetting mechanism to produce adaptive

locomotion through dynamic interactions among the body mechanical system, the nervous system, and the environment. Because cutaneous afferents were observed to contribute to these resetting behaviors [32, 117], we reset the phase ϕ_i of the oscillator i to ϕ_{AEP} when the leg i lands on the ground ($i = 1, ..., 6$). Function g_{2i} in (2.2.1) corresponds to this resetting and is given by

$$g_{2i} = (\phi_{\mathrm{AEP}} - \phi_i)\delta(t - t^i_{\mathrm{land}}), \quad i = 1, ..., 6 \tag{2.2.4}$$

where t^i_{land} is the time when the leg i contacts the ground ($i = 1, ..., 6$) and $\delta(\cdot)$ denotes the Dirac delta function. The tactile sensor signals not onlymodulate the locomotion rhythm and phase but also switch the leg movements from the swing to the stance phase, as described above.

Constraints for gait

The relative phase between the oscillators determines the gait of our robotl, which is produced by the interactions among the oscillators (2.2.3) and the sensory regulation by phase resetting (2.2.4). When we use neither (2.2.3) nor (2.2.4), the relative phase remains in the initial state and the gait does not change. When all the elements of matrix Δ^*_{ij} are determined based on the desired gait and large values are used for the gain constants K_{ij} in (2.2.3), our robot will establish the desired gait when the gait becomes stable. In contrast, when small values are used for K_{ij}, this can generate a different gait from the desired one due to the sensory regulation by phase resetting (2.2.4).

Based on the relationship of the leg movements in the locomotion of insects [132], we employed some constraints for the relative phase Δ_{ij}. Because the right and left legs move in antiphase, we used

$$\Delta^*_{21} = \Delta^*_{43} = \Delta^*_{65} = \pi \tag{2.2.5}$$

and a large value for K_{12}, K_{21}, K_{34}, K_{43}, K_{56}, and K_{65} ($K_{12} = K_{21} = K_{34} = K_{43} = K_{56} = K_{65} = 32$). In addition, because the intervals between the steps of the fore leg and middle leg and between the middle leg and hind leg are identical (they vary with the

locomotion speed), we consider

$$\Delta_{31} = \Delta_{53} \ (\Delta_{42} = \Delta_{64}) \tag{2.2.6}$$

To satisfy this condition, we modified the following desired phases using the actual relative phases by

$$\Delta^*_{31} = \Delta_{53},\ \Delta^*_{35} = \Delta_{13},\ \Delta^*_{42} = \Delta_{64},\ \Delta^*_{46} = \Delta_{24} \tag{2.2.7}$$

and used a large value for K_{31}, K_{35}, K_{42}, and K_{46} ($K_{31} = K_{35} = K_{42} = K_{46} = 40$).

From the conditions (2.2.5) and (2.2.6), $\Delta_{21} = \Delta_{43} = \Delta_{65} = \pi$ and $\Delta_{31} = \Delta_{53}$ are generally satisfied so that there are four constraints for the five state variables of the gait. Because we set the other K_{ij} to zero, the gait is determined by a single phase relationship, such as Δ_{31}, which is obtained through the locomotion dynamics. For example, our robot establishes a metachronal gait when $\Delta_{31} = 2\pi/3$ and a tripod gait when $\Delta_{31} = \pi$ (Fig. 2.4).

2.3 Result

2.3.1 Dependence of metachronal and tripod gaits on locomotion speed

We first investigated the gaits that our robot generates at $\beta = 0.62$ (v= 3.6 cm/s) and 0.7 (v = 2.5 cm/s). Specifically, we used three initial values for the relative phase Δ_{31} and examined where Δ_{31} converged.

Figure 2.5 shows the results of Δ_{31}, plotted when leg 1 touches the ground. For β = 0.62, Δ_{31} converged to 2.9 rad, indicating that our robot established the tripod gait at high speed. In contrast, Δ_{31} converged to 1.9 rad for β = 0.7, indicating that our robot performed the metachronal gait at low speed. Our robot produced different gaits depending on the locomotion speed.

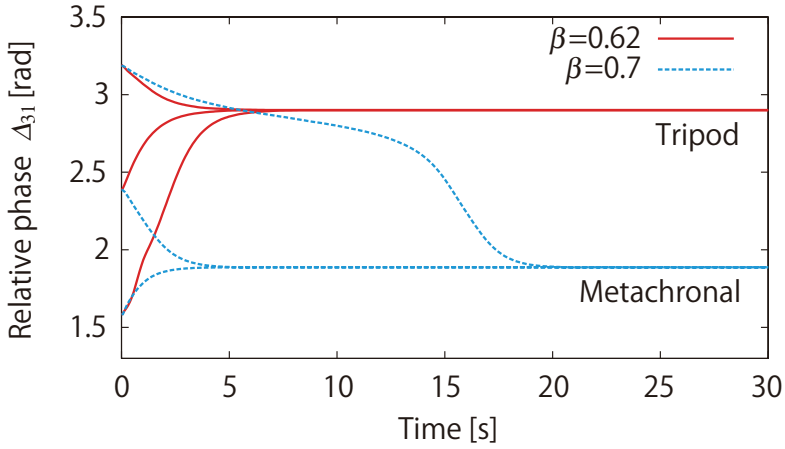

Fig. 2.5: Relative phase Δ_{31} plotted at contact of leg 1 for three initial values with $\beta = 0.62$ and 0.7. For $\beta = 0.62$ Δ_{31} converges to 2.9 rad (tripod), while Δ_{31} converges to 1.9 rad (metachronal) for $\beta = 0.7$.

2.3.2 Appearance of hysteresis in gait transition

After our robot produced a stable gait, we slowly increased the locomotion speed by reducing the duty factor β from 0.7 to 0.62 or we reduced the locomotion speed by increasing β from 0.62 to 0.7.We investigated how the gait changed through locomotion dynamics.

Figure 2.6A shows the results of Δ_{31} for increasing and decreasing the locomotion speed. It varied between 2.9 and 1.9 rad, indicating that the gait changed between the metachronal and tripod gaits. When we reduced the locomotion speed, the tripod gait transitioned to the metachronal gait at about $\beta = 0.67$. In contrast, when we increased the locomotion speed, the metachronal gait changed to the tripod gait at about $\beta = 0.645$. This means that the gait transition occurs at different locomotion speeds depending on the direction of the speed change, i.e., hysteresis appears. Figure 2.6B shows the footprint diagram during the metachronal-to-tripod gait transition.

2.3.3 Stability characteristics in the hysteresis

Based on the previous work [9], we clarify the stability structure of locomotion dynamics that induces the hysteresis in the gait transition. In particular, we use the return map of

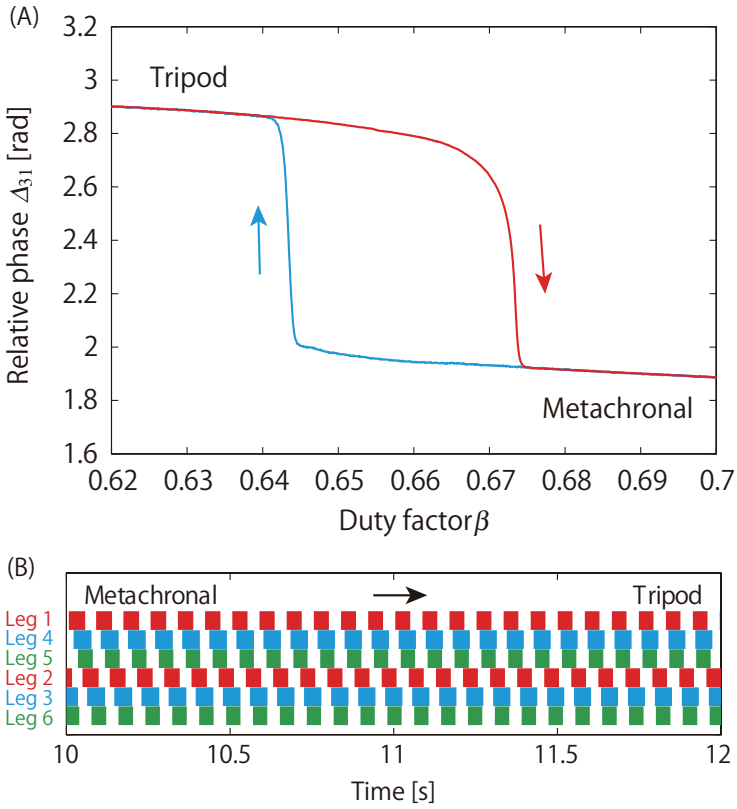

Fig. 2.6: Gait transition induced by changing the locomotion speed through duty factor β. (A) Relative phase Δ_{31}. Metachronal-to-tripod and tripod-to-metachronal gait transitions occur at different locomotion speeds and hysteresis appears. (B) Footprint diagram during metachronal-to-tripod gait transition.

Δ_{31} by plotting the relationship between Δ_{31n} at the foot contact of leg 1 for the nth gait cycle and Δ_{31n+4} for the $(n+4)$th gait cycle. We can determine possible gaits and their stabilities from the intersection with the diagonal line ($\Delta_{31n} = \Delta_{31n+4}$). Specifically, the intersection corresponds to the equilibrium point for the gait, and when the slope at the intersection is less than 1 and larger than -1, the equilibrium point is asymptotically stable. When the slope is larger than 1 or less than -1, the equilibrium point is unstable. The return map elucidates not only the local stability, but also the global stability for the gait dynamics.

Figure 2.7 shows the results of the return map for $\beta = 0.64$, 0.655, and 0.675. For $\beta = 0.64$, there is only one intersection with a diagonal line, and the tripod gait is the only attractor. When $\beta = 0.655$, three intersections appear and there are two stable

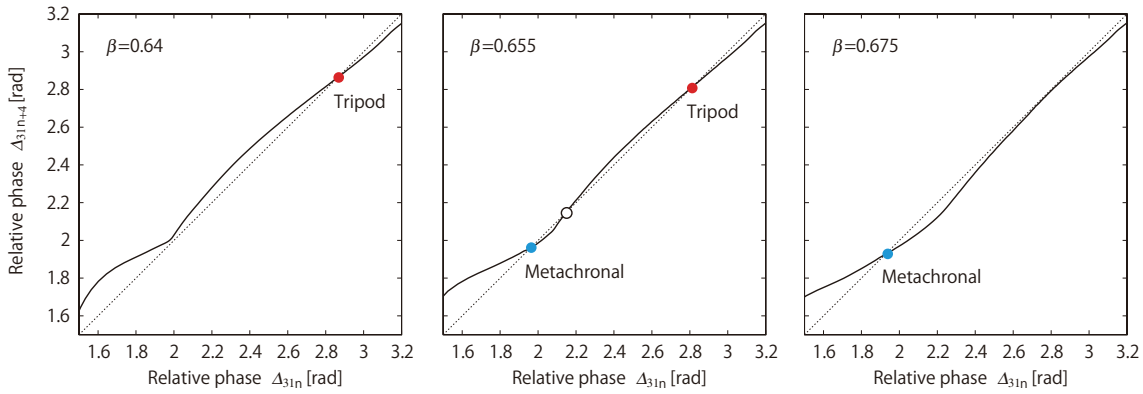

Fig. 2.7: Return maps of the relative phase Δ_{31} for $\beta = 0.64$, 0.655, and 0.675 by plotting the relationship between the relative phase Δ_{31n} for the nth gait cycle and the relative phase Δ_{31n} for the $(n + 4)$th gait cycle. Solid and open dots indicate stable and unstable gaits, respectively.

gaits (tripod and metachronal) and one unstable gait between the stable gaits (indicated by the open dot). For $\beta = 0.675$, the tripod gait disappears, which the loss of the two intersections reflects, and the metachronal gait becomes the only attractor. That is, the gait stability passes through the saddle-node bifurcation twice. A ghost appears close to the saddle-node bifurcations, as shown around $\Delta_{31n} = 2.0$ rad for $\beta = 0.64$ and Δ_{31n}= 2.8 rad for $\beta = 0.675$.

Figure 2.8 shows the stable and unstable gaits obtained by calculating the return map for each locomotion speed. The tripod gait is stable from $\beta = 0.62$ to 0.67, while the metachronal gait is stable from $\beta = 0.645$ to 0.7, indicating that two different stable gaits coexist from $\beta = 0.645$ to 0.67. These stable gaits are connected by the unstable gait, showing the fold catastrophe. These stability structures induce a jump of the gait as shown by the arrows, which give rise to the hysteresis.

2.3.4 Dependence of the gait transition on other physical conditions

In addition to the locomotion speed, we also investigated the effects of other physical conditions on the gait transition. In particular,we slowly changed themass of the body

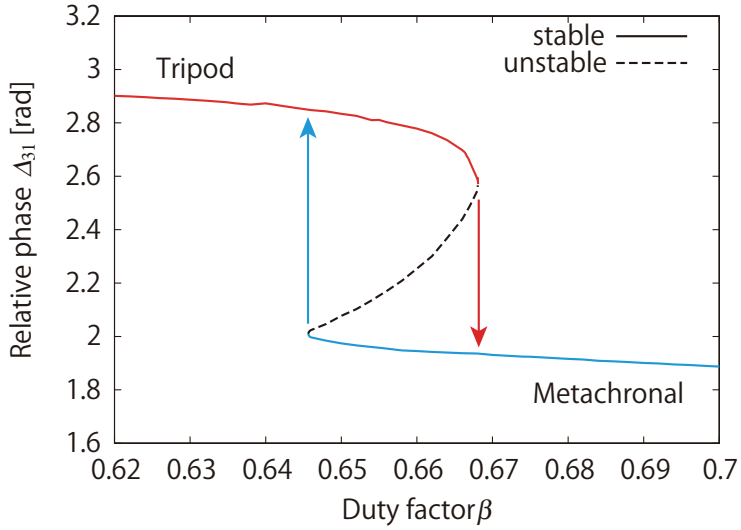

Fig. 2.8: Stable and unstable gaits calculated from the return maps. Two stable gaits and one unstable gait coexist from $\beta = 0.645$ to 0.67. Fold catastrophe occurs at connections of the stable and unstable gaits and induces jump of gaits.

or the slope angle of the ground, where we used $\beta = 0.66$, and examined what changes are induced on the gait.

Figure 2.9A shows the result of Δ_{31} when the body mass was changed. Our robot established the tripod gait for a large body mass, whereas it produced the metachronal gait for a small body mass. In addition, hysteresis occurred when the body mass was changed, as observed when the locomotion speed was changed (Fig. 2.6A).

Figure 2.9B shows the result for the change in the slope angle, where a positive slope angle indicates uphill (we used a mass of 3.0 g for the body). Our robot attained the tripod gait for uphill walking, whereas it achieved the metachronal gait for downhill walking. Hysteresis also appeared when the slope angle was changed.

Gait transitions of biological systems are affected by various physical conditions and environments. For example, when horses carry weights [36] or when they walk up an incline [131], the trot-to-gallop transition speed is reduced. Regarding the locomotion of cockroaches, while they use the tripod gait during normal walking, it changes to the metachronal gait when they are tethered on a supported ball to decrease loading [121]. Although the tripod gait remains during uphill walking, it changes to the metachronal

gait during downhill walking. Loading and uphill walking induce similar effects on their gaits [126]. Our simulation results show that only the tripod gait is stable for increased loading and the metachronal gait is stable for decreased loading (Fig. 2.9A). In addition, while the tripod gait is stable during uphill walking, it changes to the metachronal gait during downhill walking (Fig. 2.9(B)). Our results are consistent with these observations.

2.4 Discussion

In this study, we developed a neuromechanical model of an insect to emulate its dynamic locomotion. Our robot established the metachronal gait at slow locomotion speeds and the tripod gait at fast locomotion speeds, as observed in insect locomotion [29, 102, 132]. Furthermore, it exhibited a metachronal-tripod gait transition with hysteresis (Fig. 2.6). In addition to the locomotion speed, the changes in the mass of the body and the slope angle of the ground also produced the gait transition with hysteresis (Fig. 2.9). These results were not because we designed the leg movements and the locomotion control system of our robot so that it produced gait transition and hysteresis, but because the stability structure changed through dynamic interactions among the body mechanical system, the nervous system, and the environment.

The CPGs in biological systems can produce oscillatory motor commands even without rhythmic input and proprioceptive feedback. However, adequate sensory regulation of motor commands is required to generate adaptive and effective locomotion. The locomotor rhythm and phase have been shown to be modulated by producing phase shift and rhythm resetting based on sensory afferents and perturbations (phase resetting) [12, 25, 32, 113, 117]. In addition, spinal cats achieve locomotion on treadmills and their gait varies with the belt speed [40, 99], suggesting that tactile sensory information influences the locomotor rhythm and phase generated by the CPGs [32]. In this study, we used phase resetting for the sensory regulation model during locomotion. Without this sensory regulation, all the values of the relative phase Δ_{31} are neutral and the body mechanical system makes no contribution to the gait. Our sensory regulation model changed this stability structure so as to produce equilibrium points of Δ_{31}, where the

three legs are synchronized at high speeds whereas the six legs are not synchronized at low speeds. A stability analysis using the return map clarified that the equilibrium points change through the saddle-node bifurcation, which induces hysteresis in the gait transition (Fig. 2.7).

Locomotion in biological systems involves a large number of degrees of freedom. Simple physical models constructed by extracting the fundamentals of their locomotion dynamics are useful to understand their locomotor mechanism [48, 59, 61, 93, 122]. In particular, stability and bifurcation structures obtained using simple models have provided meaningful biological insights [1]. We denoted the movement of one leg by the oscillator phase and reduced the degrees of freedom of the gait by employing biologically adequate constraints, which enabled us to clarify the stability and bifurcation structures of locomotion dynamics in our robot. We intend to develop a more biomechanically and physiologically sophisticated model of insects to better understand the gait transition mechanisms in locomotion dynamics.

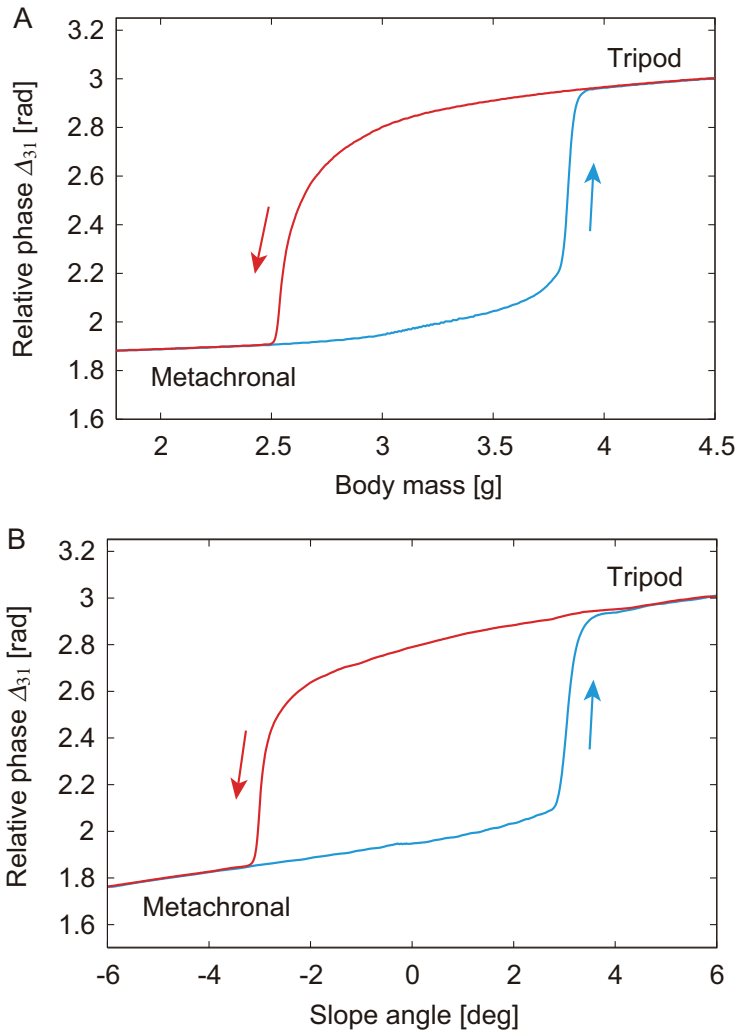

Fig. 2.9: Gait transition induced by changing (A) body mass and (B) slope angle. Positive slope angle indicates uphill. Tripod gait is produced for large body mass and uphill walking, whereas metachronal gait is generated for small body mass and downhill walking. Hysteresis appears when body mass and slope angle are changed.

Chapter 3

Splitbelt treadmill walking of a biped robot - Early adaptation

3.1 Introduction

Humans and animals are endowed with adaptive locomotion in diverse environments by cooperatively and skillfully manipulating their complicated and redundant musculoskeletal systems. In robotics research, interest in the study of legged robots has been growing. Unlike humans and animals, legged robots still have difficulties in achieving adaptive behaviors in various environmental situations. To overcome such difficulties, clarifying the mechanisms for producing adaptive functions in biological systems and constructing design principles to generate the adaptability in robotic systems are crucial issues.

In adaptive locomotor behavior, the relationship between leg movements, such as interlimb coordination, is an important factor. To investigate the mechanism controlling the interlimb coordination during walking, a special device, a splitbelt treadmill, has been used [21, 64, 88, 111, 136, 135]. The treadmill is equipped with two parallel belts. Each belt has its own motor, and thus the speeds can be controlled independently. The belts are controlled to have the same speed (tied configuration) and different speeds (splitbelt configuration) to examine how humans and animals adapt to varying environments.

Since locomotion is a well-organized motion generated through dynamic interactions between the body, the nervous system, and the environment, neuro-mechanical inter-

actions are crucial to create adaptive locomotion. To produce adaptability in various environments, the physiological concept of a central pattern generator (CPG) has been often used in the locomotion control of legged robots [35, 61, 62, 73, 85, 91, 92, 95, 123]. In our previous work, we constructed a locomotion control system using nonlinear oscillators based on this concept [7, 8]. We incorporated a phase resetting mechanism to modulate the locomotor behavior in response to sensory information based on the physiological evidence [32, 71, 113, 117] and demonstrated the adaptability of locomotion to perturbations and environmental changes, such as slopes.

Robots are effective tools for testing locomotor mechanisms with real-world dynamic characteristics [23, 61, 62, 73, 104, 112]. Otoda et al. [100] proposed an adaptation model for human splitbelt treadmill walking and investigated using a two-dimensional biped robot. They produced adaptive walking of the robot on a splitbelt treadmill by incorporating the gain adjustment of the joint feedback control. In the present study, we designed a biped robot and splitbelt treadmill and used our developed locomotion control system. We investigated the adaptability during the splitbelt treadmill walking by focusing on the functional roles of phase resetting. In addition, we measured human splitbelt treadmill walking to evaluate the adaptability in the robot. Clarifying the mechanisms producing such adaptive splitbelt treadmill walking will lead to a better understanding of the phase resetting mechanism in the generation of adaptive locomotion in biological systems and consequently to a guiding principle for designing control systems for legged robots.

This chapter is organized as follows: Sec. 3.2 introduces our experimental setup including the robot, splitbelt treadmill, and measurement of human splitbelt treadmill walking, and Sec. 3.3 addresses the locomotion control system. Section 3.4 shows the experimental results and Sec. 3.5 presents the discussion and conclusion.

Table 3.1: Physical parameters of the biped robot

Link	Mass [kg]	Length [cm]
Trunk	1.42	27.2
Arm	0.53	22.2
Leg	1.40	24.3
Total	5.28	51.5

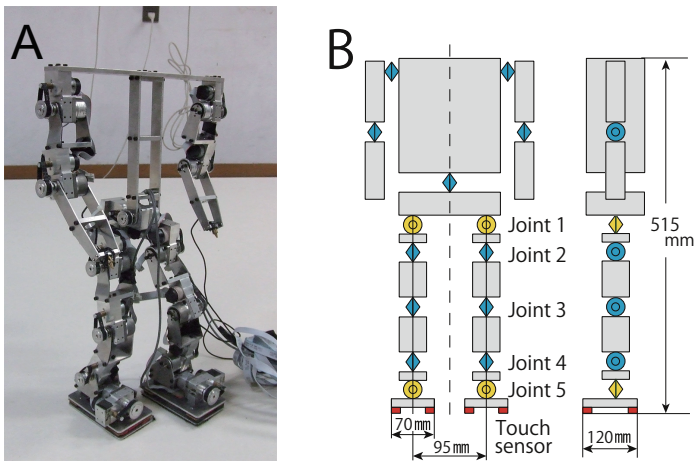

Fig. 3.1: (A) Biped robot, (B) Schematic model of the robot

3.2 Experimental setup

3.2.1 Biped robot

We used a biped robot (Figs. 3.1A, B), which consists of a trunk composed of two parts, a pair of arms composed of two links, and a pair of legs composed of five links [2]. Each link is connected to the others through a rotational joint with a single degree of freedom. Each joint is controlled by a motor, encoder (Re-max 24, Maxon motor) through a timing belt and pulleys (gear ratio 3:1) and a harmonic drive gear (gear ratio 100:1). Four touch sensors are attached to the corners of the sole of each foot. The left and right legs are enumerated as Leg 1 and 2, respectively. The joints of the legs are numbered as Joint 1

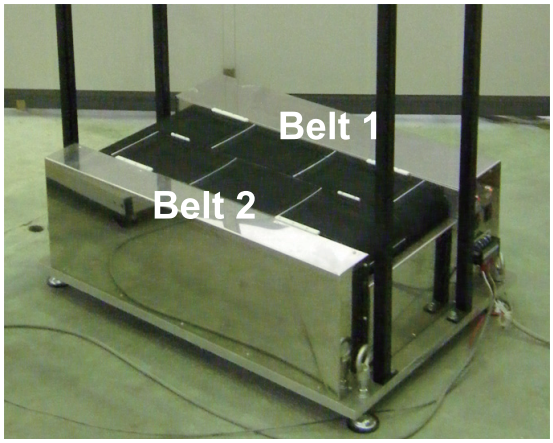

Fig. 3.2: Splitbelt treadmill for the robot.

- 5, beginning at the trunk. To describe these configurations, we introduce the angle θ_i^j ($i = 1, 2$, $j = 1, ..., 5$), which is the rotation angle of Joint j of Leg i. Table 3.1 shows the physical parameters of the robot.

Electric power is externally supplied and the robot is controlled by an external host computer (Intel Pentium 4, 2.8 GHz, RT-Linux), which calculates the desired joint motions and applies the oscillator phase dynamics in the locomotion control system (see Sec. 3.3). The system receives the command signals at intervals of 1 ms. The robot is connected with the electric power unit and the host computer by cables that are slack and held up during the experiment to avoid influencing the walking behavior.

3.2.2 Splitbelt treadmill for the robot

We developed the splitbelt treadmill, which has two parallel belts (Belts 1 and 2) and two motors with encoders (Fig. 3.2). Therefore, we can control each belt speed independently. The width of each belt is 15 cm and the distance between the rotation axes is 64 cm. The robot walks on this treadmill under various speed conditions.

Fig. 3.3: Measurement of human splitbelt treadmill walking

3.2.3 Measurement of human splitbelt treadmill walking

To investigate the adaptive functions embedded in human splitbelt treadmill walking, we measured the kinematics of a human walking on a splitbelt treadmill. The participants, who were three healthy men (ages: 22-24, weights: 51-74 kg, and heights: 163-170 cm), walked on a splitbelt treadmill (ITR3017, Bertec Corporation) and their motions were measured with a motion capture system (Digital RealTime System, Motion Analysis Corporation) (Fig. 3.3). The participants gave informed consent prior to data collection according to the procedures of the Ethics Committee of Doshisha University. Reflective markers were attached to skin of the participants over the following body landmarks on both hemibodies: ear tragus, upper limit of the acromion, greater trochanter, lateral condyle of the knee, lateralmalleolus, second metatarsal head, and heel [46]. The sampling rate was 500 Hz. Motion was recorded for the tied configuration at 3.0 km/h for both belts and the splitbelt configurations at 3.0 km/h for the right-side belt and 3.5-7.0 km/h incremented by 0.5 km/h for the left-side belt. Recording started after the participants had been walking on the treadmill long enough to settle into a regular pattern of movement for each speed condition of the splitbelt.

Humans modulate the spatiotemporal patterns of their leg movements to adapt to their environment, which, in this case, was the splitbelt treadmill. Particularly, the relative phase between the leg movements and the duty factors of the legs are modulated

depending on the speed condition [21, 88, 111]. In the present study, we focused on these adaptations. We calculated the relative phase from the measured timings of the foot-contact of the legs ((foot-contact time of slow leg − foot-contact time of fast leg)/gait cycle) and calculated the duty factors from the ratio between the foot-contact duration and the gait cycle.

3.3 Locomotion control system for the robot

3.3.1 CPG-based oscillator network model

Physiological studies have shown that the CPG in the spinal cord strongly contributes to rhythmic limb movement, such as locomotion [50, 99, 119]. The organization of the CPG remains largely undefined, although various CPG models have been proposed [53, 87]. Physiological findings suggest that the CPG consists of hierarchical networks composed of a rhythm generator (RG) and pattern formation (PF) networks [19, 71, 113, 114]. The RG network generates the basic rhythm and alters it by producing phase shifts and rhythm resetting in response to sensory afferents and perturbations (phase resetting). The PF network shapes the rhythm into spatiotemporal patterns of motor commands. That is, the CPG separately controls the locomotor rhythm and themotor commands in the RG and PF networks, respectively.

In this paper, we used the oscillator network model (Fig. 3.4), based on the two-layer hierarchical network model composed of the RG and PF networks [2, 3, 7, 8, 9], to control our robot. The RG model produces the rhythm information for locomotor behavior using phase oscillators and regulates the rhythm information by phase resetting in response to touch sensor signals. To produce the joint movements, the PF model generates motor torques based on the rhythm information from the RG model. The following sections explain the detail of the oscillator network model.

3.3.2 Rhythm generator (RG) model

The RG model produces the rhythm information for locomotor behavior through interactions of the robot mechanical system, the oscillator network system, and the environment. We used four simple phase oscillators (Leg 1, Leg 2, Trunk, and Inter oscillators), which produce the basic rhythm and phase information for locomotion based on command signals related to the locomotion speed. The oscillators also receive touch sensor signals to modulate the rhythm and phase information by phase resetting.

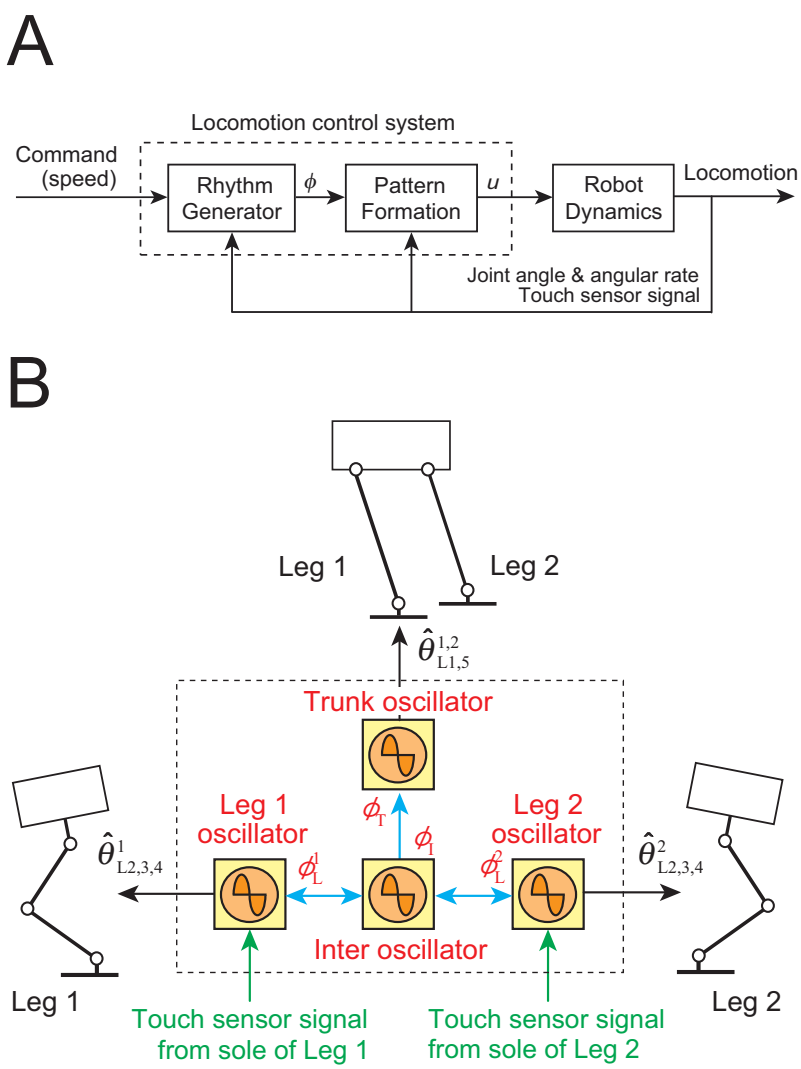

Fig. 3.4: Locomotion control system. (A) Two-layer hierarchical network model composed of a rhythm generator (RG) and pattern formation (PF) models, (B) Phase oscillators for producing locomotor rhythm and motor commands. The blue arrows indicate interactions among the oscillators. The oscillator phases are modulated by phase resetting based on touch sensor signals (green arrows). The oscillator phases determine the leg kinematics (black arrows)

We denote the phases of Leg 1 ,Leg 2, Trunk, and Inter oscillators by ϕ_1, ϕ_2, ϕ_T, and

ϕ_{I}, respectively, as given by the following dynamics

$$\begin{aligned} \dot{\phi}_{\mathrm{I}} &= \omega + g_{1\mathrm{I}} \\ \dot{\phi}_{\mathrm{T}} &= \omega + g_{1\mathrm{T}} \\ \dot{\phi}_{i} &= \omega + g^{i}_{1\mathrm{L}} + g^{i}_{2\mathrm{L}},\ i = 1, 2 \end{aligned} \tag{3.3.1}$$

where ω is the basic oscillator frequency that is the same value for all the oscillators, $g_{1\mathrm{I}}$, $g_{1\mathrm{T}}$, and $g^{i}_{1\mathrm{L}}$ $(i = 1, 2)$ are functions related to the interlimb coordination pattern (see Sec. 3.3.4), and $g^{i}_{2\mathrm{L}}$ $(i = 1, 2)$ is a function related to the phase and rhythm modulation in response to the touch sensor signals based on the phase resetting mechanism (see Sec. 3.3.5).

3.3.3 Pattern formation (PF) model

Physiological studies revealed that spinocerebellar neurons receive sensory signals from proprioceptors and cutaneous receptors and then encode the global information of the limb kinematics, such as the length and orientation of the limb axis [15, 105, 106]. We used the PF model to determine these global parameters of the leg kinematics based on the oscillator phases and produced motor torques to establish the desired kinematics.

Locomotion in humans and animals involves moving the center of mass forward. To achieve this, they move the swing leg forward. When the leg touches the ground, it supports the body and generates a propulsive force from the ground. We designed the simple leg kinematics of the swing and stance phases in reference to the length and orientation of the limb axis in the pitch plane (Fig. 3.5). The swing phase is composed of the simple closed curve of Joint 4 (ankle pitch joint), which includes an anterior extreme position (AEP) and a posterior extreme position (PEP). It starts from the PEP and continues until the foot touches the ground. The stance phase consists of a straight line from the landing position (LP) to the PEP. During this phase, the foot moves in the opposite direction to the trunk. The trunk travels in the walking direction while the foot is in contact with the ground. In both the swing and stance phases, the angular movement of Joint 4 is designed so that the foot is parallel to the line that connects

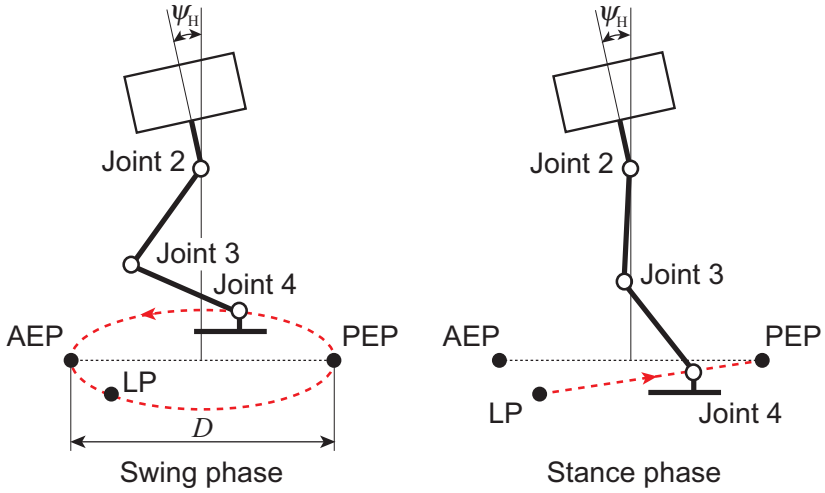

Fig. 3.5: Desired leg kinematics composed of the swing and the stance phases. When the foot lands on the ground, the trajectory changes from the swing to the stance phase. When the foot reaches point PEP, the trajectory moves into the swing phase.

points AEP and PEP. We denote D as the distance between points AEP and PEP. We denote the swing and stance phase durations by $T_{\rm sw}$ and $T_{\rm st}$, respectively, for the case that the foot touches the ground at the AEP (LP = AEP). The duty factor β, which is the ratio between the stance phase and the gait cycle, the basic frequency ω in (3.3.1), the stride length S, and the locomotion speed v are then given by

$$\begin{aligned} \beta &= \frac{T_{\rm st}}{T_{sw} + T_{\rm st}} \\ \omega &= \frac{2\pi}{T_{\rm sw} + T_{\rm st}} \\ v &= \frac{D}{T_{\rm st}} \\ S &= \frac{D}{\beta} \end{aligned} \tag{3.3.2}$$

The trunk angle $\psi_{\rm H}$ is measured from the line perpendicular to the line connecting the AEP and the PEP. The two trajectories for the swing and stance phases provide the desired motion $\hat{\theta}^i_j$ ($i = 1, 2$, $j = 2, 3, 4$) of Joint j (hip, knee, and ankle pitch joints) of Leg i by the function of phase ϕ_i of Leg i oscillator, where we use $\phi_i = 0$ at the PEP and $\phi_i = \phi_{\rm AEP} (= 2\pi(1 - \beta))$ at the AEP.

To increase the stability of bipedal locomotion in threedimensional space, we used roll joints in the legs. We designed the desired motions $\hat{\theta}^i_j$ ($i = 1, 2$, $j = 1, 5$) of Joints 1 and 5 (hip and ankle roll joints) of Leg i by the functions of phase $\phi_{\rm T}$ of Trunk oscillator by

$$\begin{aligned} \hat{\theta}^i_1 &= R\cos(\phi_{\rm T} + \varphi) \\ \hat{\theta}^i_5 &= -R\cos(\phi_{\rm T} + \varphi) \end{aligned} \tag{3.3.3}$$

where R is the amplitude of the rollmotion and φ determines the phase relationship between the leg movements in the pitch and roll planes.

Since this study focused on the adaptability of leg movements during splitbelt treadmill walking, we did not use the waist and arm movements during walking. To achieve the desired joint motions, the PF model produced motor torques based on proportional-derivative (PD) feedback control by using high-gain feedback gains by

$$\tau^i_j = -\kappa^i_j(\theta^i_j - \hat{\theta}^i_j(\phi_i)) - \sigma^i_j\dot{\theta}^i_j, \quad i = 1.2 \; j = 1, ..., 5 \tag{3.3.4}$$

where τ^i_j ($i = 1, 2$, $j = 1, ..., 5$) is the torque at Joint j of Leg i and κ^i_j and σ^i_j ($= 1, 2$, $j = 1, ..., 5$) are the gain constants.

3.3.4 Phase modulation based on the interlimb coordination pattern

The aim of this paper is to describe how our robot creates adaptive walking through dynamical interactions among the robot mechanical system, the oscillator network system, and the environment under various speed conditions of the splitbelt. In the generation of adaptive walking on a splitbelt treadmill, the interlimb coordination is a crucial factor [21, 88, 111]. Since the corresponding oscillator phase determines the desired leg kinematics, the interlimb coordination pattern of our robot is represented by the phase relationship, that is, the relative phase between the leg oscillators. Functions $g_{\rm 1I}$, $g_{\rm 1T}$, and $g^i_{\rm 1L}$ in (3.3.1) modulate this interlimb coordination and are given as follows by using

the relative phase between the oscillators based on Inter oscillator,

$$\begin{aligned} g_{1\mathrm{I}} &= -\sum_{i=1}^{2} K_{\mathrm{L}} \sin(\phi_{\mathrm{I}} - \phi_i + (-1)^i \pi/2) \\ g_{1\mathrm{T}} &= -K_{\mathrm{T}} \sin(\phi_{\mathrm{T}} - \phi_{\mathrm{I}}) \\ g^i_{1\mathrm{L}} &= -K_{\mathrm{L}} \sin(\phi_i - \phi_{\mathrm{I}} - (-1)^i \pi/2), \quad i = 1, 2 \end{aligned} \tag{3.3.5}$$

where K_{L} and K_{T} are gain constants. These interactions are shown by the blue arrows in Fig. 3.4B. Depending on the gain parameter K_{L}, these functions move the phase relationship between the legs into the desired state in which both legs move in antiphase with each other; $\phi_1 - \phi_2 = \pi$. Therefore, when we use a large value for K_{L}, $\phi_1 - \phi_2 = \pi$ is satisfied. In contrast, when we use a small value for K_{L}, the relative phase between the leg oscillators is shifted from antiphase through the phase regulation by the phase resetting shown below.

3.3.5 Phase modulation based on phase resetting

Although the CPG can produce oscillatory signals even in the absence of rhythmic input and proprioceptive feedback, it must use sensory feedback to create adaptive and effective locomotor behavior. For example, spinal cats produce locomotor behaviors on a treadmill and their gait changes depending on the belt speed [40, 99]. This result suggests that the tactile sensory information between their feet and belt influences the locomotion phase and its rhythm generated by the CPG [33]. Physiological studies have shown that the locomotion rhythm and its phase are modulated by producing phase shift and rhythm resetting based on sensory afferents and perturbations (phase resetting) [25, 32, 54, 71, 117]. In addition, the functional roles of phase resetting in the generation of adaptive walking have been investigated using neuromusculeskeletal models [5, 6, 134, 137, 138].

We modulated the locomotion rhythm and its phase based on the phase resetting mechanism in response to touch sensor signals in order to create adaptive locomotor behavior through dynamic interactions between the robot mechanical system, the oscillator network system, and the environment. Function $g^i_{2\mathrm{L}}$ in (3.3.1) corresponds to this mod-

ulation. When Leg i lands on the ground, phase ϕ_i of Leg i oscillator is reset to ϕ_{AEP} $(i = 1, 2)$. Therefore, function $g^i_{2\mathrm{L}}$ is written by

$$g^i_{2\mathrm{L}} = (\phi_{\mathrm{AEP}} - \phi_i)\delta(t - t^i_{\mathrm{land}}), \quad i = 1, ..., 6 \tag{3.3.6}$$

where t^i_{land} is the time when Leg i lands on the ground $(i = 1, 2)$ and $\delta(\cdot)$ denotes Dirac's delta function. Note that the touch sensor signals not onlymodulate the locomotor rhythm and its phase but also switch the leg motions from the swing phase to the stance phase, as described in Sec. 3.3.3 (this does not induce a discrete change in the desired leg kinematics). Also note that this phase resetting does not work for Trunk and Inter oscillators, but only for the leg oscillators.

3.3.6 Parameter determination

The locomotion control system has the following parameters: D, T_{sw}, and T_{st} to determine the locomotion speed (3.3.2), ψ_{H}, R, and φ to determine the leg movements in the pitch (Fig. 3.5) and roll plane (3.3.3), and K_{T} and K_{L} to determine the strength of the interaction among the oscillators (3.3.5). In particular, the synchronization of the roll and pitchmotions during locomotion is crucial to produce stablewalking. We used R and φ for the rollmotion and ψ_{H} for the pitchmotion as tuning parameters [7]. Since K_{L} is crucial to control the interlimb coordination pattern, we investigated the roles of this parameter in the generation of adaptive walking (see Sec. 3.4.3). It should be noted that this study does not focus on the optimality of these parameters, but the emergence of adaptive functions during locomotion through interactions of the robot mechanical system, the oscillator network system, and the environment.

3.4 Results

3.4.1 Generation of walking under various speed conditions

To investigate how our robot establishes adaptive walking on the splitbelt treadmill, we used two conditions for the speeds of the left-side belt v_1 and the right-side belt v_2: 1. a

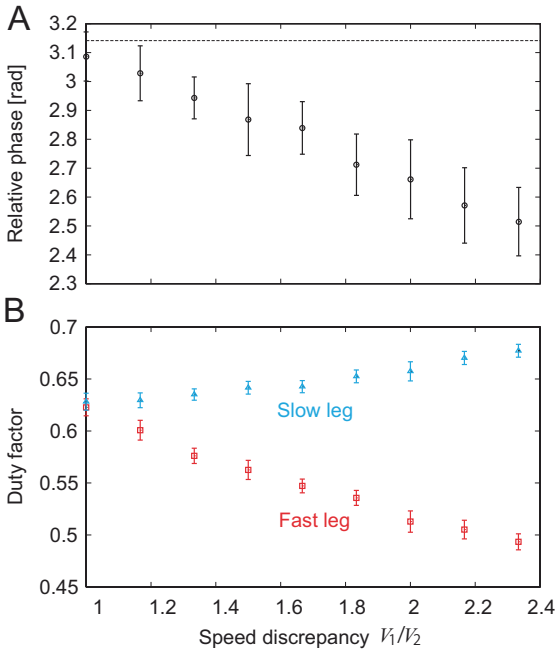

Fig. 3.6: Adaptation in human splitbelt treadmill walking. (A) Relative phase between the leg movements, and (B) Duty factors. V_1 and V_2 are the speeds of the left-side and right-side belts, respectively.

tied configuration, $v_1 = v_2$, and 2. a splitbelt configuration, $v_1 > v_2$, similarly to the measurement of human splitbelt treadmill walking. We examined only the configuration ($v_1 > v_2$) because the robot mechanical system has bilateral symmetry. We used the following parameters, which are independent of the speed conditions of the splitbelt: D = 2.5 cm, $T_{\rm sw}$ = 0.35 s, $T_{\rm st}$ = 0.35 s, $R = 3°$, $\varphi = -170°$, $\phi_{\rm H} = 5°$, $K_{\rm T}$ = 10, and $K_{\rm L}$ = 1.0. Given these parameters, β = 0.5, S = 5 cm, and v = 7.1 cm/s in (3.3.2). To clearly see the differences among various speed conditions, the robot first walked in the tied configuration. After the robot established steady walking, we changed the speed condition of the treadmill from the tied to the splitbelt configuration and examined howthe robot adapted to the changed environment.

When we did not use phase resetting, the robot easily fell down. However, the robot with phase resetting achieved steady and straight walking on the splitbelt treadmill without changing the control parameters, indicating that the robot established dynamically stable walk due to phase resetting. One foot of the robot contacted only the ipsilateral

belt during locomotion, even when one belt speed was 2.0 times faster than the other belt speed (v_1 = 9.3, v_2 = 4.6 cm/s). When the speed discrepancy between the belts was larger than this, the robot did not fall down but it was difficult for it to establish a straight walk for a long time.

3.4.2 Adaptive behaviors in splitbelt treadmill walking of human and robot

Humans generate adaptive walking on a splitbelt treadmill, because they can change both the relative phase between leg movements and the duty factors depending on the speed condition [21, 88, 111]. We measured human splitbelt treadmill walking, as shown in Fig. 3.6. This figure shows the relative phase and the duty factors for various speed conditions, where the data points and error bars correspond to the means and standard deviations of over 50 gait cycles. Although the data shown were obtained from one participant, the other participants showed similar trends. As the speed discrepancy between the belts increased, the relative phase shifted from antiphase and the duty factors on the fast belt decreased whereas the duty factors on the slow belt increased.

To investigate why our robot generated steady walking on a splitbelt treadmill, as shown in the previous section, we examined the relative phase between the leg oscillators $\phi_1 - \phi_2$ and the duty factors of the legs. Figure 3.7 shows the representative result after we changed the speed condition from the tied configuration ($v_1 = v_2$ = 6.9 cm/s) to the splitbelt configuration (v_1 = 8.5, v_2 = 5.4 cm/s). For the tied configuration shown in Fig. 3.7A, although the relative phase fluctuates discretely due to phase resetting, it remains approximately π rad. This means that the two legs moved in antiphase with each other during locomotion. However, for the splitbelt configuration, the average of the phase difference slightly shifted from π rad, indicating that the phase relationship between the leg movements changed from antiphase due to the discrepancy between the belt speeds. Figure 3.7B shows the duty factors of the legs during locomotion. Although the legs have almost the same values in the tied configuration, the values are slightly different for the splitbelt configuration.

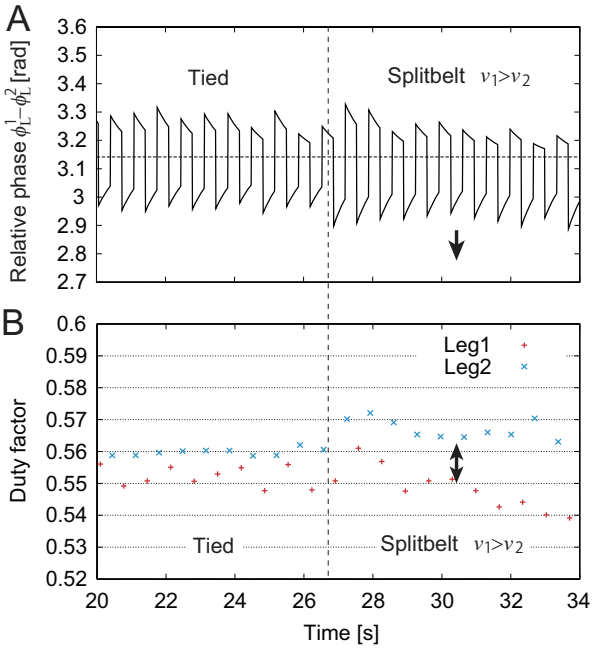

Fig. 3.7: Changes in relative phase and duty factors by changing the speed condition from the tied configuration ($v_1 = v_2$) to the splitbelt configuration ($v_1 > v_2$). (A) Relative phase $\phi_1 - \phi_2$, and (B) Duty factors. The speed condition changes are denoted by the vertical dotted line.

To more clearly see these effects, we conducted thorough investigations using various conditions of belt speeds. Figure 3.8 shows the changes of the relative phase between the leg oscillators from the tied configuration to the splitbelt configuration (A) and the changes of the duty factors (B) due to the speed discrepancy between the belts. The values are the averages over five gait cycles for each trial. The data points and error bars correspond to the means and standard deviations of the five experiments. This figure clearly shows that the relative phase shifted from π rad and that the duty factors changed depending on the speed discrepancy between the belts. These trends are similar to those observed in human splitbelt treadmill walking (Fig. 3.6).

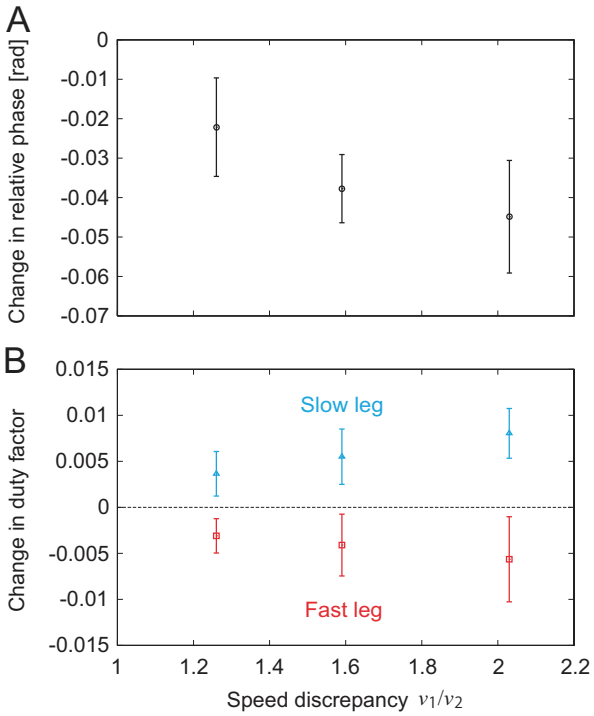

Fig. 3.8: Changes from the tied configuration to the splitbelt configuration versus the discrepancy between the belt speeds v_1/v_2. (A) Relative phase between the leg oscillators, and (B) Duty factors. The data points and error bars correspond to the means and standard deviations of five experiments.

3.4.3 Contribution of phase modulations based on phase resetting and interlimb coordination pattern

The relative phase between the leg oscillators is determined by the interaction among the oscillators (3.3.5) and the phase regulation by the phase resetting (3.3.6). When we use neither (3.3.5) nor (3.3.6), the relative phase never changes from the initial value. When we use a large value for the gain parameter K_{L} in (3.3.5), the relative phase hardly shifts from antiphase. In contrast, when we use a small value for K_{L}, the relative phase can shift from antiphase. That is, the relative phase depends on the relationship between the interaction among the oscillators (3.3.5) and the phase regulation by phase resetting (3.3.6).

To investigate this effect on the production of adaptive splitbelt treadmill walking, we used various values for K_{L} and examined how much belt speed discrepancy the robot

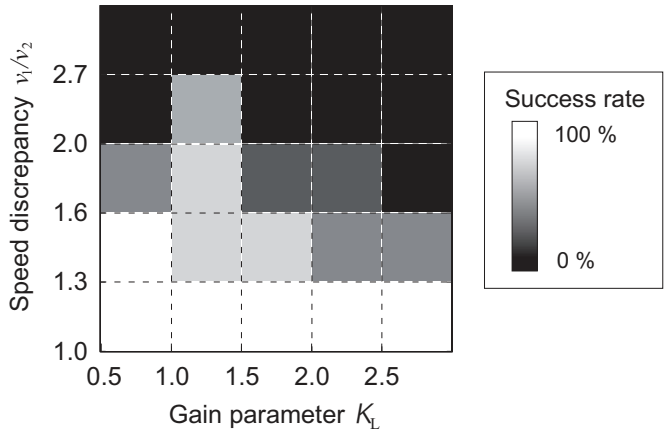

Fig. 3.9: Success rate of splitbelt treadmill walking for various speed conditions and values of K_{L}. The lower left corner of each box corresponds to the axis value.

can adapt to for each K_{L}. We used 0.5-2.5 incremented by 0.5 for K_{L} and four splitbelt configurations, (v_1, v_2) = (7.7, 6.2), (8.5, 5.4), (9.3, 4.6), and (10.1, 3.8 cm/s). We used the same values for the parameters of the locomotion control system as in the previous sections except for K_{L}. We considered a trial to be successful if the robot walked in a straight line for 15 steps in the manner that one foot contacts only the ipsilateral belt during walking after the configuration changes from the tied to the splitbelt configuration. For each K_{L} and splitbelt configuration, we performed the robot experiment five times and examined the success rate. Figure 3.8 shows the result. The larger the speed discrepancy of the belts, the lower the success ratewas for each K_{L}. The success rate depended on K_{L}, and we obtained the best success rate for $K_{\mathrm{L}} = 1.0$.

Next, to investigate why the success rate depended on K_{L}, as shown in Fig. 3.9, we examined the changes of the relative phase between the leg oscillators and the duty factors from the tied to the splitbelt configuration for some values of K_{L}. The changes were calculated by averaging five gait cycles for each trial, as in Fig. 3.8. Figure 3.10 shows the changes in the relative phase (A) and the duty factors (B), for $K_{\mathrm{L}} = 0.5$, 1.0, and 1.5, where $v_1 = v_2 = 6.9$ cm/s for the tied configuration, and $v_1 = 7.7$ and $v_2 = 6.2$ cm/s for the splitbelt configuration. The larger the value we used for K_{L}, the smaller were the changes of the relative phase and the duty factors. When we used a large value for K_{L}, the interaction among the oscillators (3.3.5) remained strongly in the relative phase

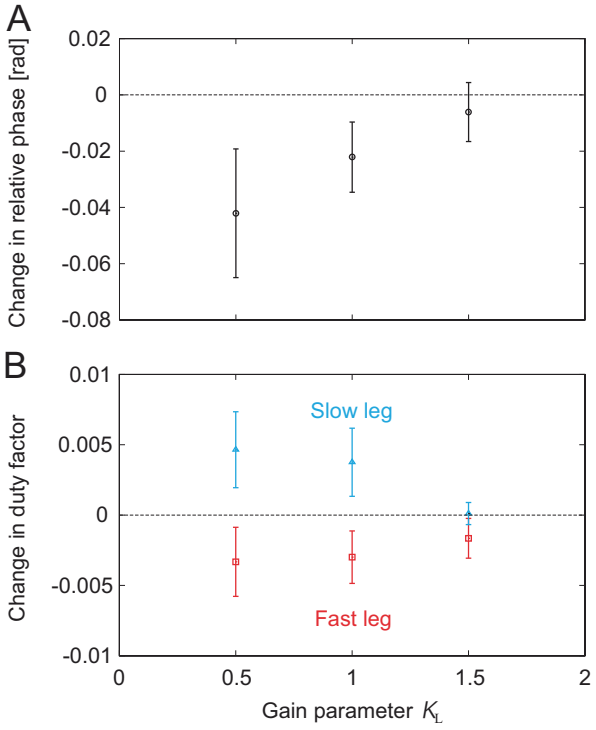

Fig. 3.10: Changes from the tied configuration to the splitbelt configuration versus the discrepancy between the belt speeds v_1/v_2. (A) Relative phase between the leg oscillators, and (B) Duty factors. The data points and error bars correspond to the means and standard deviations of five experiments.

π rad, and the relative phase did not vary from π rad, even with the modulation of the phase resetting. At the same time, the leg movements were constrained to be antiphase and the duty factors scarcely changed. Hence, it was difficult for the robot to walk in a straight line in the environment that the belt speeds are different. When we used a small value for K_{L}, the interaction among the oscillators (3.3.5) became smaller, and the relative phases were allowed to vary from π rad due to phase resetting (3.3.6). The relative phase between the leg movements shifted from antiphase and the duty factors changed greatly. However, the fluctuation became large and decreased the stability for walking in a straight line.

3.5 Discussion

In general, environmental variations, such as the speed discrepancy between the belts, decreases the locomotion stability of the biped robot, unless the robot changes the control strategy or control parameters to cope with such variations. However, our robot established stable walking without changing the control strategy and parameters, despite a large discrepancy between the belt speeds. Instead, the relative phase between the leg movements shifted from antiphase and the duty factors of the legs varied depending on the speed discrepancy between the belts (Figs. 3.7, 3.8). This is because the speed discrepancy between the belts caused changes in the locomotion dynamics. More specifically, it yielded changes in the timing of the foot contact for each leg. For example, since the stance leg on the belt with a faster speed is pulled more backward than the contralateral leg, the robot falls forward and the foot contacts of the contralateral leg occur earlier. Such temporal asymmetry shifts the relative phase of the leg oscillators due to phase resetting and modulates the phase relationship between the leg movements, and therefore creates spatial asymmetry of the locomotor behaviors. These locomotor behaviors can be verified from the changes in the foot patterns (Fig. 3.11). Human splitbelt treadmill walking showed similar trends. These temporal and spatial asymmetries reflect the adaptability achieved during splitbelt treadmill walking. This adaptability in our robot is not a characteristic that we specifically designed, but it emerged through the dynamic interactions of the robot mechanical system, the oscillator control system, and the environment. When the robot movements are completely predetermined, as in the case without phase resetting (Sec. 3.4.1), the robot cannot establish such adaptability and easily falls down.

Although physiological evidence has shown that the locomotor rhythm and its phase are modulated by producing a phase shift and rhythm resetting based on sensory afferents and perturbations [25, 32, 71, 117], such rhythm and phase modulations in phase resetting have for the most part been investigated for fictive locomotion in cats, and their functional roles during actual locomotion remain largely unclear. Simulation studies with neuromusculeskeletal models of biological systems have shown the functional

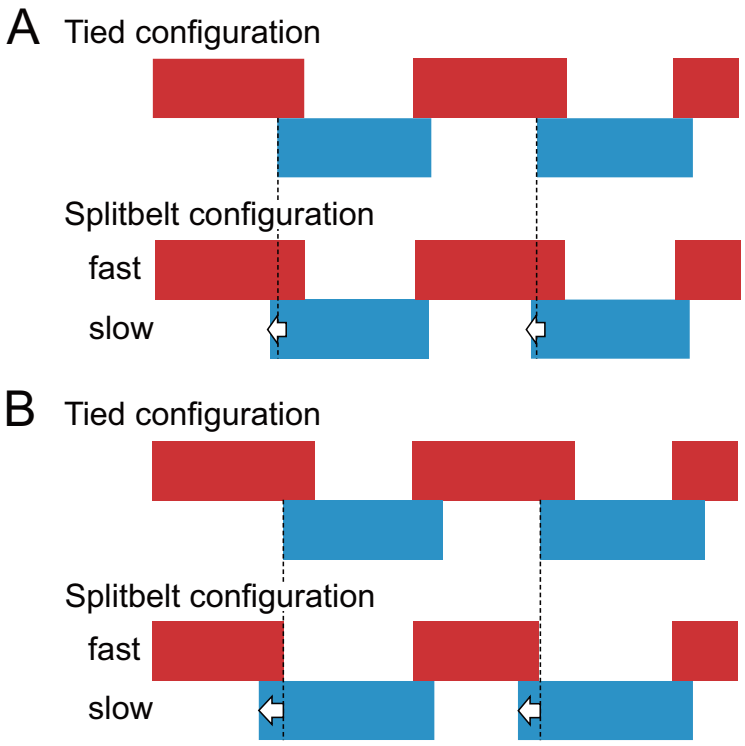

Fig. 3.11: Foot patterns of tied and splitbelt configurations. (A) Robot with $v_1 = 8.5$ and $v_2 = 5.4$ cm/s, and (B) Human with $V_1 = 7.0$ and $V_2 = 3.0$ km/h. The bold lines indicate the foot-contact duration.

roles of phase resetting in the generation of adaptive walking [4, 5, 6, 134, 137, 138]. Our results regarding the improvement of the adaptability in locomotion through temporal modulation by phase resetting, as obtained in our robot experiments, are consistent with the simulation results of biological systems.

To create adaptive splitbelt treadmill walking, the controls of the locomotor rhythm and its phase for each leg as well as the relative phase between the legs are crucial. Our results show that the phase regulation by the interaction among the oscillators and the phase resetting should be well-balanced (Figs. 3.9, 3.10), which is the same as the previously reported simulation result of a physiologically based model of human walking [5].

So far, phase resetting has been demonstrated to be useful in the generation of adaptive locomotion of biped robots to perturbations and environmental changes, such as slopes [2, 7, 8, 91, 92, 95]. Our results show that phase resetting contributes to the spe-

cial environment of the splitbelt treadmill without incorporating special techniques. This further clarifies the usefulness of phase resetting in the generation of adaptive locomotion of legged robots and can lead to further progress in the design of a locomotion control system.

To clearly investigate the adaptive functions of phase resetting in splitbelt treadmill walking, we used simple robot kinematics and a simple control strategy. We did not use any vision or gyro sensors to regulate postural behaviors. We used only touch sensors to recognize the environmental situation and to modulate the robot movements. Therefore, the adaptability of our control system is limited. However, the shifts of the relative phase between leg movements and the modulations of the duty factors of the legs were observed during human splitbelt treadmill walking (Fig. 3.6), and our results suggest that our simple dynamic model using the robot with the oscillator control system reflects the essence of the ability to produce adaptive locomotor behaviors.

Although we investigated steady walking behaviors on the splitbelt treadmill, two types of adaptation can be found in human splitbelt treadmill walking when switching the configurations of the splitbelt [21, 88, 111]. One is early adaptation, which quickly modulates the locomotor behavior to adapt to the changed environment. The other is late adaptation, which slowly modulates the locomotor behavior through learning to produce a new pattern and induces aftereffects. Since we did not incorporate any learning mechanism in our locomotion control system, our robot does not produce such slow adaptation and aftereffects. In the next chapter, we intend to improve our locomotion control system to investigate this adaptation mechanism in human splitbelt treadmill walking and to produce further design principles for the control systems of legged robots.

Chapter 4

Splitbelt treadmill walking of a biped robot - Late adaptation

4.1 Introduction

Humans have ability to walk adaptively in various environments by producing motor commands appropriately in their neural system. Because humans generate their walking behavior through the movements of many joints, they have to create proper relationships of the movements between the legs (interlimb coordination) and between the joints in a leg (intralimb coordination) depending on the environmental situation. However, it remains unclear how humans control such interlimb and intralimb coordinations during walking, which attracts many researchers.

To investigate the underlying mechanism in the interlimb and intralimb coordinations in locomotion of humans and animals, splitbelt treadmills have been often used [21, 28, 42, 69, 88, 89, 108, 135, 136]. It has two parallel belts, whose speeds are controlled independently, and artificially creates left-right symmetric and asymmetric environments for walking using tied cofiguration (same speed between the belts) and splitbelt configuration (different speeds between the belts). During the tied configuration, the left and right legs move in anti-phase and have similar motions, as observed during overground walking. However, soon after changing to the splitbelt configuration, characteristic locomotion parameters, such as the relative phase between the legs, duty factor, and center

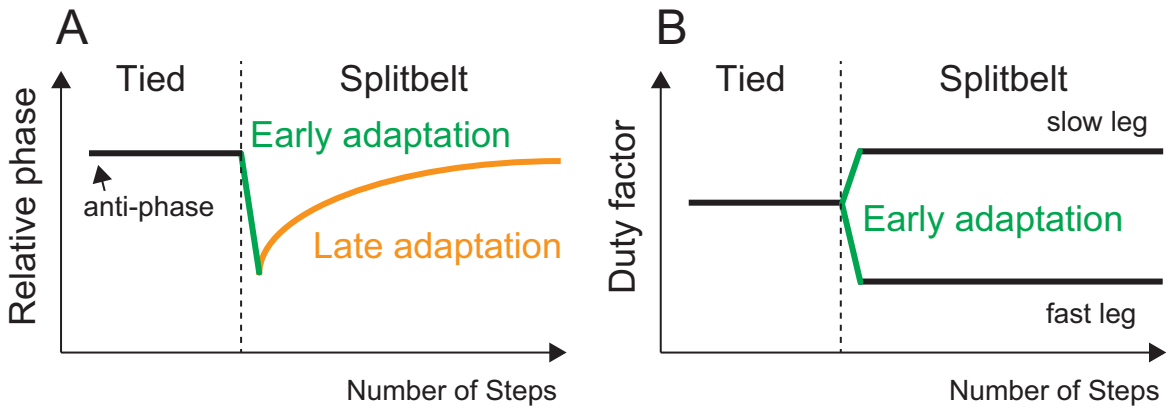

Fig. 4.1: Changes in (A) relative phase between legs and (B) duty factor of legs in human splitbelit treadmill walking (modified from [111]). When speed condition changes from tied to splitbelt configuration, these values rapidly change (early adaptation); relative phase shifts from anti-phase and duty factor of fast leg decreases whereas that of slow leg increases. After a while, relative phase gradually returns to anti-phase (late adaptation) whereas duty factors remain.

of pressure (COP) profile, rapidly change. This rapid change is called early adaptation. Moreover, by continuing to walk on this condition, locomotion parameters related to the interlimb coordination, such as the relative phase and COP profile, gradually change and have a trend to return to the state in the tied configuration, whereas locomotion parameters related to the intralimb coordination, such as the duty factor, do not show further adaptation. This gradual change in the interlimb coordination is called late adaptation.

More specifically about the early and late adaptations, the relative phase rapidly changes from anti-phase at the early adaptation and gradually returns to anti-phase again for the late adaptation (Fig. 4.1A) [111]. The duty factor of the fast (slow) leg rapidly decreases (increases) at the early adaptation, but it does not show further change during the splitbelt configuration (Fig. 4.1B). The COP profile shows a butterfly pattern for one gait cycle, whose wings are symmetric during the tied configuration (Fig. 4.2A) [86]. At the early adaptation, the wing of fast (slow) side rapidly moves backward (forward) (Fig. 4.2B). For the late adaptation, the wings gradually move so that their center positions return to the original positions and become identical (Fig. 4.2C).

Early adaptation of locomotion parameters has been observed during splitbelt tread-

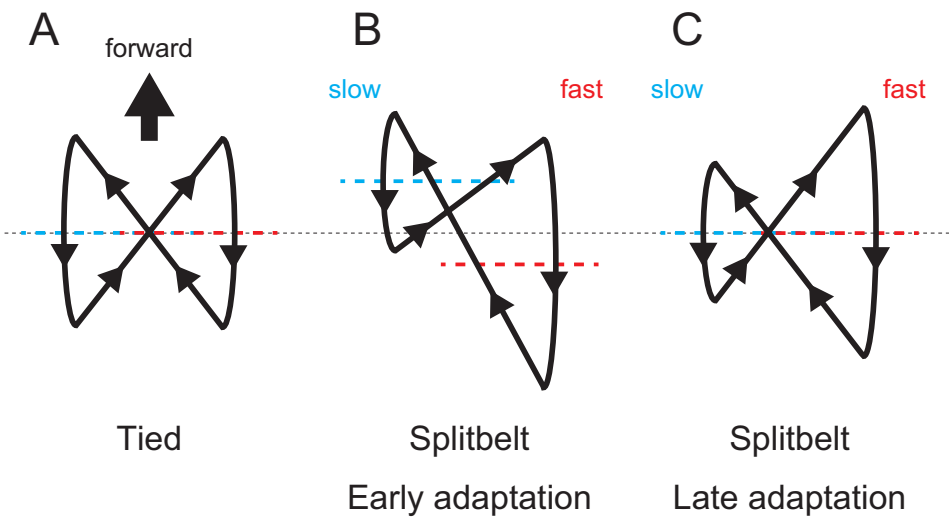

Fig. 4.2: Change in butterfly pattern of center of pressure profile in human splitbelit treadmill walking (modified from [86]). Dotted lines show center of each butterfly wing. In (A) tied configuration, butterfly wings and their centers are identical between legs. In (B) early stage of splitbelt configuration, butterfly wing of slow leg moves forward whereas that of fast leg moves backward. In (C) late stage of splitbelt configuration, centers of butterfly wings return to original position.

mill walking of spinal cats [42, 41], which suggests that sensorimotor integration in the spinal cord induces the early adaptation. On the other hand, humans with cerebellar damage do not show late adaptation during splitbelt treadmill walking, which suggests that cerebellum contributes to late adaptation. However, it remains unclear how neural information processing induces such adaptations.

To reveal the contribution of neural processing to adaptation of walking, analytical approaches using measured data and observation of humans have limitation. To overcome it, constructive approaches using physical models and robots have been attracted [44, 62, 80, 100, 125]. In particular, neuromechanical models, which integrate neural control model and body mechanical model, have been used to examine physiological hypothesis related to motor control during walking. In the previous work [45], we developed a simple locomotion control model of the spinal cord as a neural control model for walking based on the physiological concept of central pattern generator (CPG) and sensory reflex related to foot contact, and performed experiments using a biped robot walking on a splitbelt

treadmill as a body mechanical model. The result showed that the robot established stable walking during both the tied and splitbelt configurations without changing the control strategy and parameters, despite large discrepancy between the belt speeds in the splitbelt configuration. Instead, the relative phase between the legs shifted from anti-phase and duty factors changed depending on the speed discrepancy between belts, similarly to early adaptation in humans. These adaptive behaviors were not because we specifically designed in our control model, rather than because the phases of the leg motions were automatically modulated by immediately responding to the changes of foot contact timings due to the speed discrepancy of the left-right belts of the treadmill. However, because the locomotion control model did not include a function to regulate motor commands by the cerebellum, gradual change of locomotion parameters in late adaptation was not observed, and our model did not fully explain the adaptation in human splitbelt treadmill walking.

It is suggested that the cerebellum predicts sensory consequences of movement based on the efference copy and modifies motor commands through learning based on the error information between the predicted and actual sensory information [94]. The experiments of walking on a surface with an unexpected hole showed that the absence of sensory afferent about foot contact at the appropriate timing triggeres a behavior like reflexive reaction [56, 129], which suggests that the foot contact event is predicted during walking. Furthermore, during the splitbelt treadmill walking, left-right foot contact timings actually change depending on the speed condition of the treadmill [79]. In this study, we incorporate a cerebellar model to our spinal locomotion control model, which modulates the foot contact timing of each leg through learning only using local sensory information about foot contact of each leg. We conducted computer simulation and robot experiment of a biped robot walking on a splitbelt treadmill. Our results show that despite no direct control of the inter limb coordination, late adaptation appears in the inter limb coordination similarly to humans, which was evaluated by measuring human splitbelt treadmill walking. In addition, we clarify the adaptation mechanism from a dynamic viewpoint.

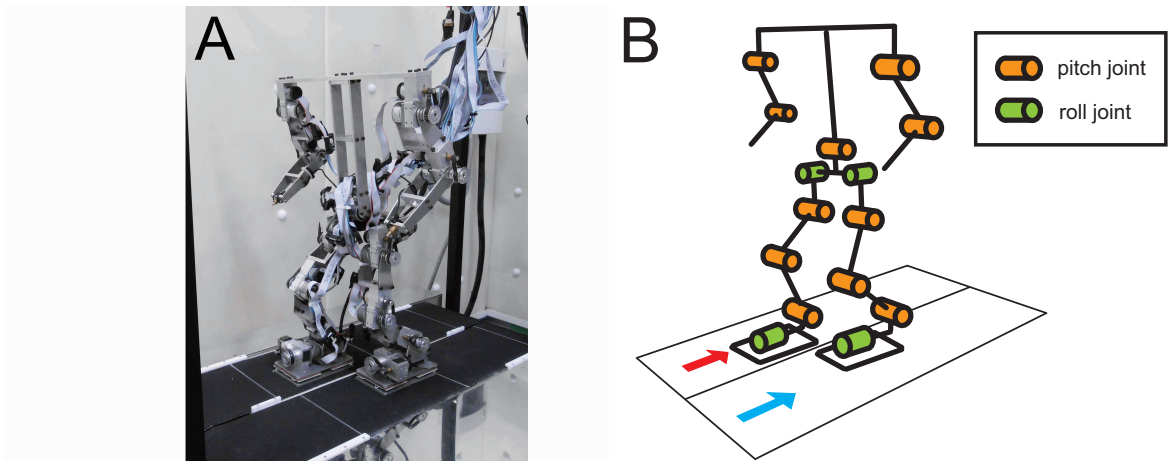

Fig. 4.3: Experimental setup. (A) Biped robot and splitbelt treadmill and (B) schematic model.

4.2 Materials and methods

4.2.1 Mechanical setup of robot experiment

Biped robot

In this study, we used a biped robot (Fig. 4.3) developed in the previous work [2]. It consists of a trunk composed of two parts, a pair of arms composed of two links, and a pair of legs composed of five links. Each link is connected to the others through a rotational joint with a single degree of freedom. The hip has pitch and roll joints, the knee has a pitch joint, and the ankle has pitch and roll joints. Each joint is manipulated by a motor with an encoder. Four touch sensors are attached to the corners of the sole of each foot. We denote the right and left legs by Legs 1 and 2. The robot was cont rolled by an external host computer (Intel Core i5, real-time embedded Linux Xenomai) with 0.2 ms intervals and the electric power was supplied externally. The robot was connected with the host computer and the electric power unit by cables, which were slack and held up during the experiment to avoid influencing the locomotor behavior.

For the computer simulation, we used a physical model whose configuration and physical parameters were based on those of the robot. To simulate the locomotor behavior of the robot model, we derived the equations of motion using Lagrangian equations as

in [2, 9]. We performed forward dynamic simulation by solving the equations of motion using a fourth-order Runge-Kutta method with a step size of 0.1 ms.

splitbelt treadmill for the robot

For the robot experiment, we used a splitbelt treadmill (Fig. 4.3), which was developed in our previous work [45]. It has two parallel belts, each of which is equipped with a motor and an encoder to control individual belt speed. The width of each belt is 15 cm and the distance between the rotation axes is 64 cm.

To simulate the walking of the robot model on a splitbelt treadmill, we used two separate floors that move parallel and independently. We modeled the foot contact with the floor by vertical viscoelastic elements and horizontal viscous elements.

4.2.2 Biologically inspired spinal and cerebellar locomotion control model

We developed a locomotion control model composed of two layers (Fig. 4.4,4.5); spinal model, which produces motor commands to manipulate the robot based on CPG and sensory reflex, and cerebellum model, which modulates the motor commands through learning.

Spinal CPG model

The spinal CPG model was developed in the previous work [2, 3, 45] to emulate the sensorimotor properties in the spinal CPG to produce adaptive locomotion. To show the relationship of the spinal CPG and cerebellar learning models, we briefly explain the spinal CPG model.

The CPG is suggested to consist of a two-layered hierarchical network composed of a rhythm generator (RG) and pattern formation (PF) networks [19, 113]. The RG network generates the basic rhythm and alters it by producing phase shifts and rhythm resetting in response to sensory afferents (phase resetting). The PF network shapes the rhythm into spatiotemporal patterns of motor commands. Based on this physiological finding,

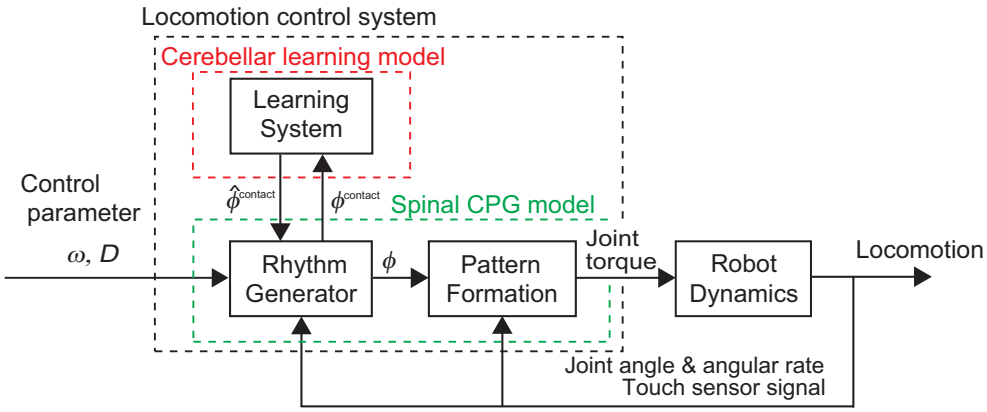

Fig. 4.4: Locomotion control model composed of spinal CPG and cerebellar learning models. Spinal CPG model consists of rhythm generator (RG) and pattern formation (PF) models. Cerebellar learning model receives phase information of foot contact timing from RG moodel and sends desired (predicted) foot contact timing to RG model.

we developed the spinal CPG model by the following RG and PF models.

For the RG model, we used four simple phase oscillators (Leg 1, Leg 2, Trunk, and Inter oscillators), whose phases are denoted by ϕ_1, ϕ_1 , $\phi_{\rm T}$, and $\phi_{\rm I}$. The oscillator phases follow the dynamics

$$\begin{aligned}
\dot{\phi}_i &= \omega - K_{\rm I}\sin(\phi_i - \phi_{\rm I} - (-1)^i\pi/2) + (\hat{\phi}_i^{\rm contact} - \phi_i^{\rm contact})\delta(t - t_i^{\rm contact}) \; i = 1, 2 \\
\dot{\phi}_{\rm I} &= \omega - K_{\rm T}\sin(\phi_{\rm T} - \phi_{\rm I}) \\
\dot{\phi}_{\rm T} &= \omega - \sum_{i=1}^{2} K_{\rm I}\sin(\phi_{\rm I} - \phi_i + (-1)^i\pi/2)
\end{aligned} \tag{4.2.1}$$

where ω is the basic oscillator frequency, $\delta(\cdot)$ is Dirac delta function, and $K_{\rm I}$ and $K_{\rm T}$ are gain parameters. The second terms of the right hand side of each equation represent the interaction among oscillators to move the relative phase between the leg oscillators into antiphase. Note that we used a small value for $K_{\rm I}$ so that the relative phase can be shifted from anti-phase by phase resetting and learning through locomotion dynamics. The third term of the right hand side of the equation for the leg oscillators represents phase resetting. Inspired from spinal cats walking on a treadmill showing that foot contact information influences the locomotion phase and rhythm generated by the CPG [33],

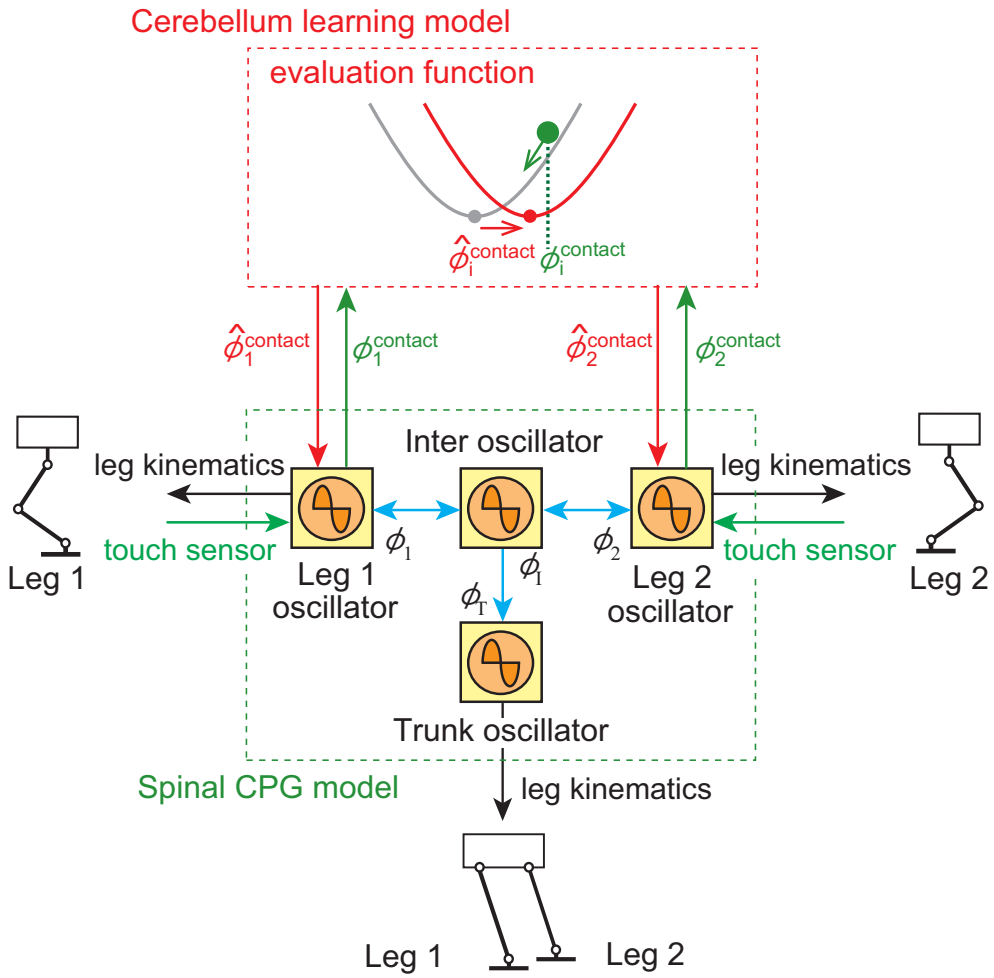

Fig. 4.5: Locomotion control model to show the function of each phase oscillator in spinal CPG model and learning in cerebellar model. Blue arrows indicate interactions among oscillators. Oscillator phases are modulated by phase resetting based on touch sensor signals and desired (predicted) foot contact timing (green arrows). Oscillator phases determine leg kinematics (black arrows). Cerebellar learning model receives phase information at foot contact (green arrows) and modifies desired (predicted) foot contact timing using evaluation function, which is sent to spinal CPG model (red arrows).

we modulated the oscillator phase in response to touch sensor signals based on phase resetting. More specifically, when the leg i ($i = 1, 2$) touched the ground at the time t_i^{contact}, the phase of the leg i oscillator ϕ_i^{contact} is reset to $\hat{\phi}_i^{\text{contact}}$. This Jiontact corresponds to the desired (predicted) foot contact timing, as explained later.

For the PF model, inspired from the physiological finding that spinocerebellar neurons encode the global information of the limb kinematics, such as the length and orientation of the limb axis [15, 105, 106], we produced motor commands to achieve the desired leg kinematics of the robot, which was determined based on the oscillator phases from the RG model. We used a simple leg kinematics in reference to the length and orientation of the limb axis in the pitch plane, which consists of the swing and stance phases (Fig. 4.6). The swing phase is a simple closed curve of the ankle pitch joint, which includes an anterior extreme position (AEP) and a posterior extreme position (PEP). It starts from the PEP and continues until the foot contact. The AEP corresponds to the desired foot contact position. The stance phase is a straight line from the contact position (CP) to the PEP. These two trajectories for the swing and stance phases are given as function of the corresponding oscillator phase, where $\phi_i = 0$ at the PEP and $\phi_i = \hat{\phi}_i^{\text{contact}}$ at the AEP. We denote D as the distance between the AEP and PEP, and T as the gait cycle ($\omega = 2\pi/T$). The desired duty factor $\hat{\beta}$, stride length $\hat{S}$, and locomotion speed $\hat{v}$ are then given by

$$\begin{aligned} \hat{\beta} &= 1 - \frac{\hat{\phi}_i^{\text{contact}}}{2\pi} \\ \hat{S} &= \frac{D}{\hat{\beta}} \\ \hat{v} &= \frac{D}{\hat{\beta} T} \end{aligned} \tag{4.2.2}$$

To increase the locomotion stability in three dimensional space, we also used the hip and ankle roll joints using simple sinusoidal functions based on the trunk oscillator. Because we focused on the adaptive behavior of the leg motions on the splitbelt treadmill walking, we did not use the waist and arm movements. To generate the desired kinematics, each joint is controlled by the joint torque based on PD feedback control.

Cerebellar learning model

The cerebellum involves motor learning, where it receives efference copy of motor commands and sensory afferents and modifies the motor commands based on these infor-

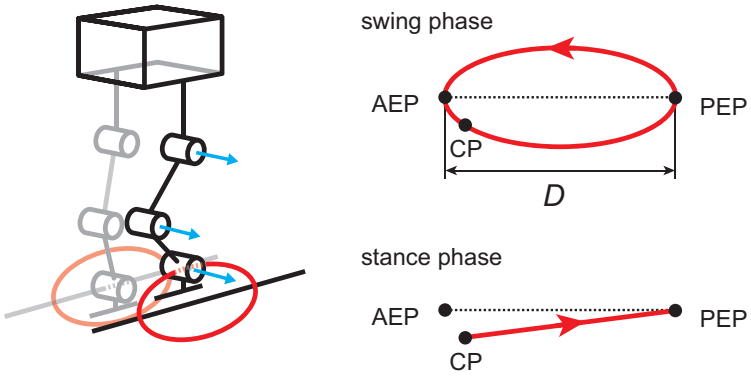

Fig. 4.6: Desired leg kinematics composed of the swing and the stance phases. When foot lands on ground at contact point (CP) (anterior extreme position (AEP) is desired foot contact position), trajectory changes from swing to stance phase. When foot reaches posterior extreme position (PEP), trajectory moves into swing phase.

mation [110, 133]. It predicts the sensory consequences of the movement based on the efference copy and evaluates if the motor commands are appropriate based on the error information between the predicted and actual sensory information [13]. The cerebellum modifies the motor commands through learning to reduce the error.

It is suggested that the cerebellum predicts the timing of sensory events [94, 98] and contributes to achieving the task which needs accurate temporal control [66, 67, 120]. Moreover, it is reported that the damage to the cerebellum impairs the temporal accuracy during the motor learning despite not the spatial accuracy [16]. The experiments of walking on a surface with an unexpected hole showed that the absence of sensory afferent about foot contact at the appropriate timing referring to the prediction triggeres a behavior like reflexive reaction [56, 129], which suggests that the predict ion of foot contact timing is important for motor learning in walking. Furthermore, during the splitbelt treadmill walking, the foot contact timing actually change depending on the configuration of the treadmill [79], which also suggests the importance of the prediction and modulation of foot contact timing.

In this study, we focus on foot contact timing for the cerebellar learning model. In particular, we modulate the desired (predicted) foot contact timing $\hat{\phi}_i^{\text{contact}}$ through learning based on the error between the predicted and actual foot contact timing. We

define an evaluation function $V_{i,n}$ for the nth step of the Leg i using the error between the desired (predicted) foot contact phase $\hat{\phi}_{i,n}^{\text{contact}}$ and actual foot contact phase $\phi_{i,n}^{\text{contact}}$ for the nth step of the Leg i, which is given by

$$V_{i,n} = \frac{1}{2}(\hat{\phi}_{i,n}^{\text{contact}} - \phi_{i,n}^{\text{contact}})^2 \tag{4.2.3}$$

Based on this evaluation function, we predict the next foot contact timing. More specifically, from the gradient direction of the evaluation function, $\hat{\phi}_i^{\text{contact}}$ is modulated by

$$\hat{\phi}_{i,n+1}^{\text{contact}} = \hat{\phi}_{i,n}^{\text{contact}} - \alpha \frac{\partial V_{i,n}}{\partial \hat{\phi}_{i,n}^{\text{contact}}} \tag{4.2.4}$$

where α is the learning rate. Because $\hat{\phi}_{i,n}^{\text{contact}}$ corresponds to the desired timing of the corresponding leg to switch from the swing to stance phase, this temporal modulation changes the desired duty factor of the corresponding leg (4.2.2) and makes the CP identical to the AEP in Fig. 4.6.

4.2.3 Robot experiment

For the robot and simulation experiments, we used the following control parameters; D = 2.5 cm, T = 0.6 s, K_{I} = 1.0, K_{T} = 10, and α= 0.35. For the initial value of $\hat{\phi}_i^{\text{contact}}$, we used π, which gives $\hat{\beta}$ = 0.5, $\hat{S}$ = 5.0 cm, and $\hat{v}$ = 8.3 cm/s. We did not change the control parameters, irrespective of the speed condition of the treadmill.

For the splitbelt treadmill, we denote the speed of the left belt by v_1 and that of the right belt by v_2 At the beginning, the robot walked in the tied configuration using v_1 = v_2 = 7.9 cm/s. After the robot established steady walking, we suddenly changed the speed condition from the tied to splitbelt configuration using v_1= 9.7 and v_2 = 6.1 cm/s. For the robot experiment, we performed this trial five times and investigated the robot behavior from the average of the results.

4.2.4 Measurement of human splitbelt treadmill walking

To evaluate the biological relevance of our findings from the robot and simulation experiments, we measured human walking on a splitbelt treadmill (ITR3017, Bertec Corporation) that has two separate belts and an embedded force plate underneath. The participants, who were five healthy men (ages: 22-24, weights: 51-74 kg, and heights: 163-170 cm), held onto a bar on the front of the treadmill and wore a safety harness with cords which were slack and suspended during the experiment so that they do not affect the locomotor behavior. The participants gave informed consent prior to data collection according to the procedures of the Ethics Committee of Doshisha University.

Each trail consists of five sessions based on the previous work [111] (Fig.4.7) and each participant conducted one trail. In the first session, the participants walked with the tied configuration using $v_1 = v_2 = 0.5$ m/s for two minutes. In the second and third sessions, they walked with the tied configuration using $v_1 = v_2 = 2.0$ m/s and $v_1 = v_2 = 0.5$ m/s, respectively, for two minutes again. In the forth session, they walked with the splitbelt configuration using $v_1 = 0.5$ and $v_2 = 2.0$ m/s for ten minutes. In the final session, they walked with the tied configuration againt using $v_1 = v_2 = 0.5$ m/s for six minutes. Time interval between sessions was at most one minute, just enough to change the speed condition of the treadmill. Their kinematics was measured with a motion capture system (Mac 3D Digital RealTime System, Motion Analysis Corporation). The sampling rate of the motion capture and the force plate was 500 Hz. Reflective markers were attached to skin of the participants over the head, back, and both hemibodies of upper limit of the acromion, elbow, hand, greater trochanter, lateral condyle of the knee, lateralmalleolus, second metatarsal head, and heel. The measured kinematic and force data were low-pass filtered at 6 Hz (with a second-order Butterworth filter). The COP was computed using the force and kinematic while center of mass (COM) was computed using kinematic data. To see the COP relative to the body, we used COM projected on the ground for the origin of the coordinate and computed COP − COM.

As Mawase et al. [86] showed, the COP profile changes during human splitbelt treadmill walking (Fig. 4.2). This change reflects the change in the stride and step lengths shown by Reisman et al. [111], because the stride length is related to the vertical length

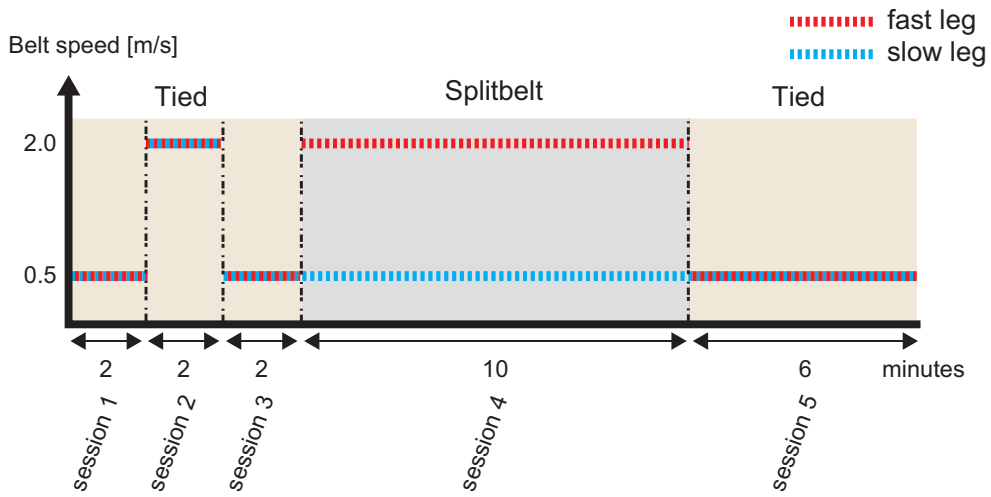

Fig. 4.7: Experimental protocol of human splitbelt treadmill walking composed of five sessions. Session 1 is slow tied configuration for two minites, session 2 is fast tied configuration for two minutes, session 3 is slow tied configuration for two minutes, session 4 is splitbelt configuration for ten minutes, and session 5 is slow tied configuration for six minutes.

of the butterfly wing of the COP and the step length is related to the relative position of the two wings. The remarkable point is the change of the center position of the butterfly wings in the COP pattern. More specifically, their centers are identical between the legs during the tied configuration. However, soon after the splitbelt configuration starts, the slow side moves forward, whereas the fast side moves backward. After a while, they return to the original position and become identical again. That is, the relative position between the centers of the wings change depending on the configuration and stage of the speed condition of the treadmill. In this study, to clearly show this change, we investigated the left-right difference of the center of the butterfly wings of the COP pattern. For statistical analysis, we used averages of first five steps in the session 1 for the tied configuration, and first and last five steps in the session 4 for the early and late stages, respectively, of the splitbelt configuration, where we used measured COP data of each participant by normalizing using the mean stride length in the tied configuration. We used one-way repeated-measures ANOVA to compare differences between the three testing intervals (tied configuration and early and late stages of splitbelt configuration), When the ANOVA showed significant difference, we used post hoc analysis using Tukey's

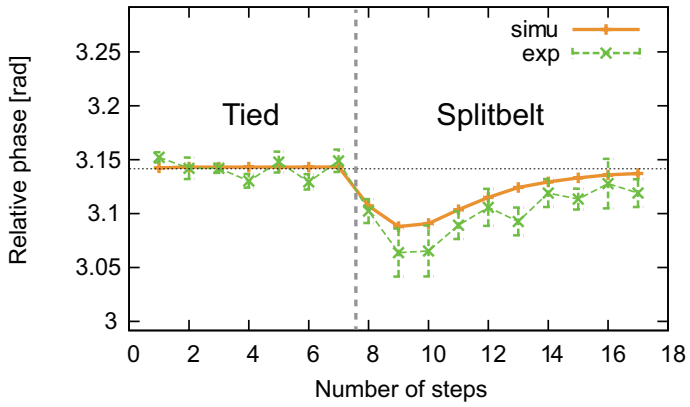

Fig. 4.8: Relative phase between leg oscillators for simulation and robot experiments. For the robot experiment, the data points and error bars are means and standard errors of results of five experiments. During tied configuration, relative phase is anti-phase. Soon after changing to splitbelt configuration, it rapidly shifted. After a while, it gradually returned.

honestly significant different test.

4.3 Results

4.3.1 Relative phase between the legs

Figure 4.8 shows the relative phase between the leg oscillators, which corresponds to the relative phase between the legs, for the computer simulation and robot experiment using the average value for one gait cycle by $\frac{1}{T}\int_T(\phi_1-\phi_2)dt$. For the robot experiment, the data points and error bars are means and standard errors of the results of five experiments. During the tied configuration, the relative phase shows anti-phase. However, soon after changing to the splitbelt configuration, it rapidly shifted from anti-phase. After a while, it gradually returned to anti-phase.

Figure 4.9 shows the amount of phase resetting ($\hat{\phi}_i^{\text{contact}} - \phi_i^{\text{contact}}$) at foot contact whose square value corresponds to the evaluation function $V_{i,n}$ for learning. When this amount is positive (negative), the foot contact occurs earlier (later) than the predicted timing. This amount is almost zero at the tied configuration, but appeared soon after the splitbelt configuration started. After a while, it converged to zero again, meaning that

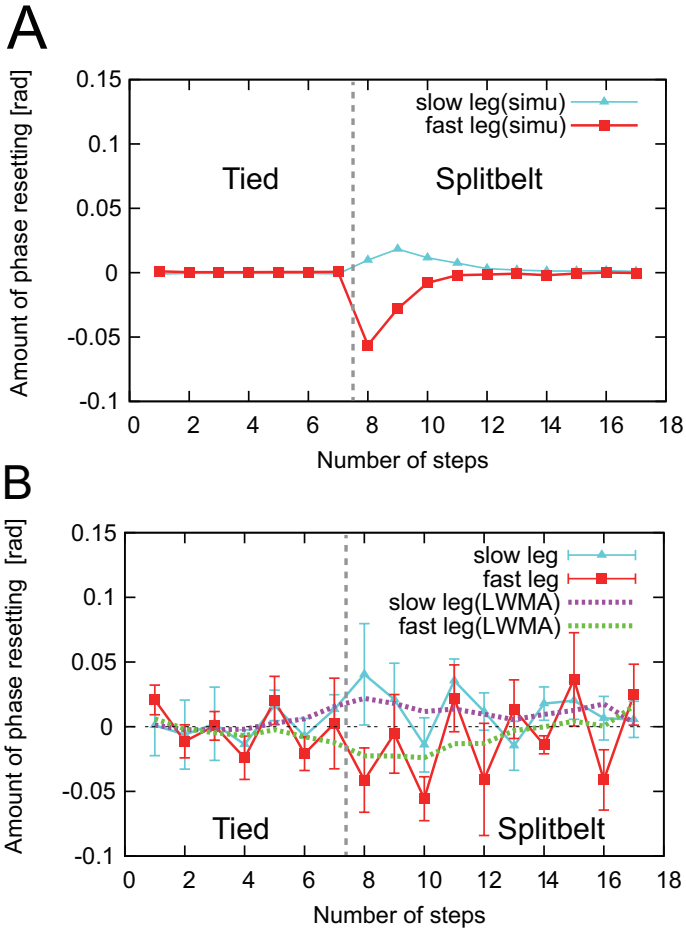

Fig. 4.9: Amount of phase resetting of leg oscillators for (A) simulation and (B) robot experiments. For robot experiment, data points and error bars are means and standard errors of results of five experiments, and dotted lines are five-period linear weighted moving average (LWMA). Amount of resetting was zero during tied configuration, but appeared soon after chaning to splitbelt configuration. After a while, it gradually converged to zero again.

the learning was completed. Although the robot experiments have disturbance for this amount, the moving average (five-period linear weighted moving average) clearly shows this property.

The results of the robot and simulation experiments are qualitatively and quantitatively similar. Moreover, the relative phase has a qualitatively similar trend to the early and late adaptations of human splitbelt treadmill walking (Fig. 4.1A).

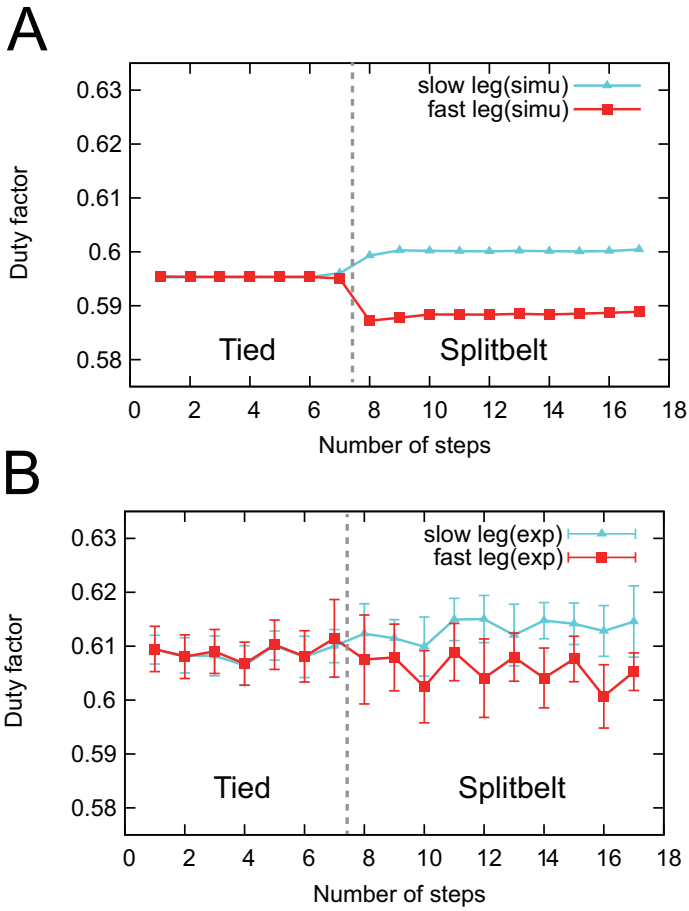

Fig. 4.10: Duty factors of legs for (A) simulation and (B) robot experiments. For robot experiment, data points and error bars are means and standard errors of results of five experiments. Duty factors were identical between legs during t ied configuration. They rapidly changed soon after splitbelt configuration started. They remained after rapid change.

4.3.2 Duty factors

Figure 4.10A and B show the duty factors of the legs for the computer simulation and robot experiment, respectively. For the robot experiment, the data points and error bars are means and standard errors of the results of five experiments. During the tied configuration, the duty factors were identical between the legs. Soon after changing to the splitbelt configuration, the duty factor of the fast leg rapidly decreased, while that of the slow leg increased. They remained after the rapid changes unlike the relative phase between the legs (Fig. 4.8).

Although the duty factors of the robot experiment were slightly larger than those

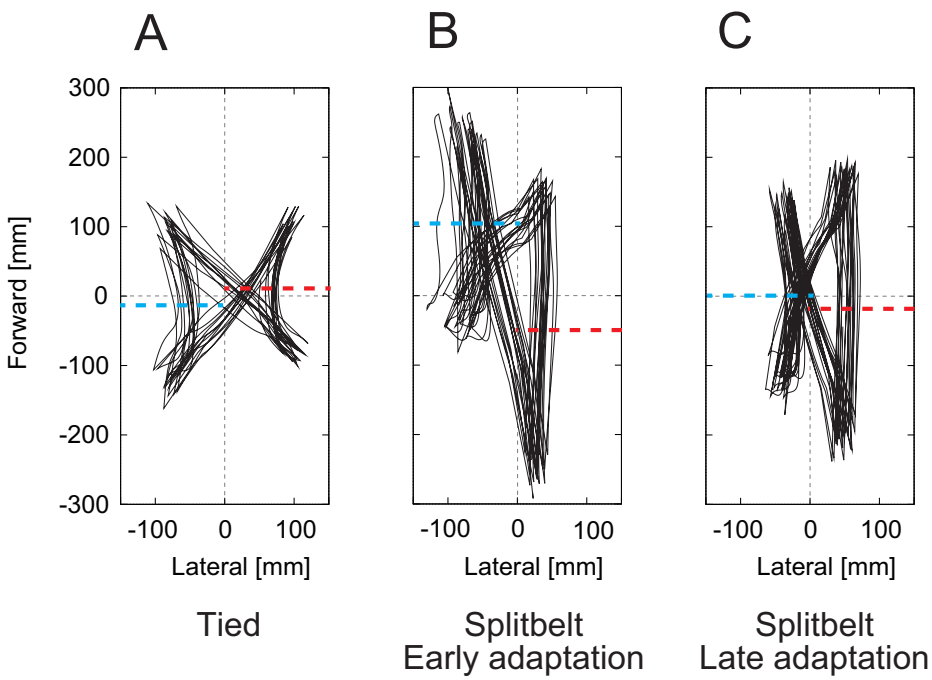

Fig. 4.11: Center of pressure profile relative to center of mass measured during human splitbelt treadmill walking for (A) tied configuration (first 20 s of session 1), (B) early stage of splitbelt configuration (first 20 s of session 4), and (C) late stage of splitbelt configuration (last 20 s of session 4).

of the computer simulation, the results of the robot and simulation experiments have a qualitatively and quantitatively similar trend. Furthermore, the results of the duty factors have a qualitatively similar trend in human splitbelt treadmill walking (Fig. 4.1B), similarly to the relative phase between the legs.

4.3.3 Center of pressure

Figure 4.11A, B, and C show the COP profile of one participant using the data of first 20 s during the tied configuration of the first session, the data of first 20 s during the splitbelt configuration of the fourth session, and the data of last 20 s of the fourth session, respectively. During the tied configuration, the butterfly wings of the COP pattern were almost identical between the legs, so did their center positions (Fig. 4.11A). Soon after the start of the splitbelt configuration, the wing of the slow side moved forward and that

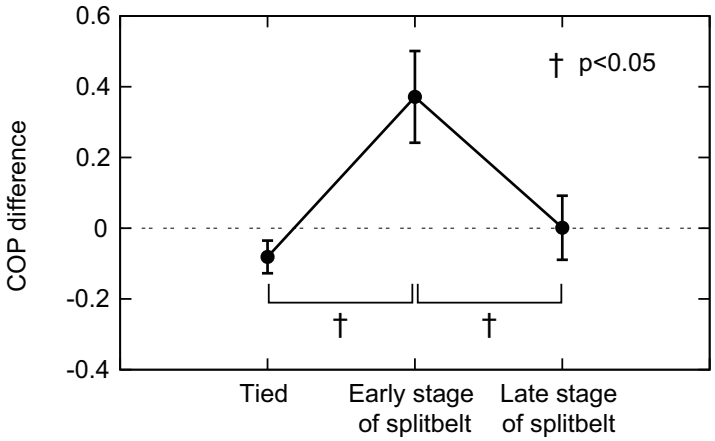

Fig. 4.12: Left-right difference of center of butterfly wings of COP pattern of five participants for three intervals (tied, early stage of splitbelt, and late stage of splitbelt configurations). Positive value indicates that slow side is forward than fast side. Data points and error bars are means and standard errors of five participants. During tied configuraion, difference was almost zero (center position was almost identical between legs). Difference appeared in early stage of splitbelt configuration, but reduced to be almost zero again in late stage of splitbelt configuration.

of the fast side moved backward (Fig. 4.11B). After a while, they moved so that their center positions became identical again (Fig. 4.11C). These features are consistent with the report by Mawase et al. [86].

To clearly show this change for all participants, we investigated the left-right difference of the center of the butterfly wings. Figure 4.12 shows the means and standard errors of the results of five participants for the tied, early stage of splitbelt, and late stage of splitbelt configurations. In the tied configuration, the difference was almost zero, meaning that the center position was almost identical between the legs. The difference occurred in the early stage of splitbelt configuration, but reduced to be almost zero again in the late stage of splitbelt configuration. There was a significant main effect for periods ($P < 0.05$) from the ANOVA, and the post hoc testing revealed that the difference of the center of the wings changed from the tied configuration to the early stage of splitbelt configuration ($P < 0.05$) and from the early stage of splitbelt configuration to the late stage of splitbelt configuration ($P < 0.05$). However, the difference between the tied configuration and the late stage of splitbelt configuration was very little and significant

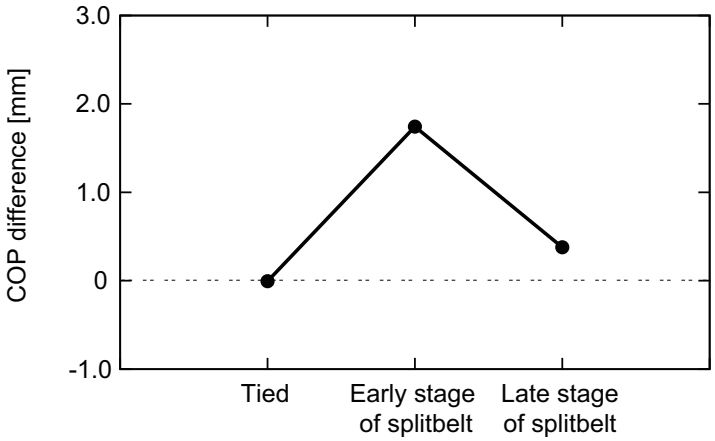

Fig. 4.13: Simulation result of left-right difference of center of butterfly wings of COP pattern for three intervals (tied, early stage of splitbelt, and late stage of splitbelt configurations). Positive value indicates that slow side is forward than fast side. During tied configuraion, difference was zero (center position was identical between legs). Difference occurred in early stage of splitbelt configuration, but decreased to be almost zero again in late stage of splitbelt configuration.

difference could not be found ($P > 0.3$).

Figure 4.13 shows the result of the computer simulation for the difference of the center of the butterfly wings of the COP pattern. During the tied configuration, there was no difference between the legs. The difference appeared at the early stage of splitbelt configuration, but decreased to be almost zero again at the late stage of splitbelt configuration. These trends are qualitatively similar to those in human splitbelt treadmill walking (Fig. 4.12).

4.4 Discussion

4.4.1 Adaptation mechanism from a dynamic viewpoint

In this study, we developed a control model of spinal cord and cerebellum for walking based on physiological findings; for the spinal model, we determined motor commands using an oscillator network based on the CPG while incorporating sensory reflex based on foot contact information and for the cerebellar model, we modified the motor commands

based on the error information between the predicted and actual foot contact timings through learning. We performed the robot and simulation experiments of a biped robot on a splitbelt treadmill to investigate what adaptatioin appears and what mechanism explains the adaptation. Our results showed that characteristic locomotion parameters, such as the relative phase between the legs and duty factors, show similar trend to early and late adaptations in human splitbelt treadmill walking.

As Reisman et al. [111] pointed out, only the locomotion parameters involved in the interlimb pattern change gradually in the late adaptation of human splitbelt treadmill walking. Our results of the adaptation were induced by the sensory reflex and learning only using local information about foot contact of each leg. Despite no direct control of the interlimb coordination in the model, our robot showed similar characteristics in the early and late adaptations of the interlimb coordination. We discuss the adaptation mechanism from a dynamic viewpoint below.

Foot contact timing of the slow (fast) leg becomes earlier (later) when the speed condition changes from the tied to splitbelt configuration, as reported by MacLellan et al. [79]. This change is induced by the change of the pitching moment of the body in the sagittal plane due to the speed discrepancy of the belts. More specifically, during the tied configuration, the pitching moment is identical between the legs (Fig. 4.14A). Soon after the splitbelt configuration starts, the pitching moment of the fast leg increases during the single support phase due to the increase of the belt speed to pull the fast leg (Fig. 4.14B), which induces early foot contact of the contralateral (slow) leg. Similar mechanism is also applied to the other side and foot contact of the fast leg is delayed. These changes in the foot contact timing are verified from the amount of phase resetting in our model (Fig. 4.9) and induced the shift of the relative phase between the legs from anti-phase in the early adaptation (Fig. 4.8).

During the late adaptation, the difference of the pitching moment between the legs reduces due to the gradual modulation of the foot contact timing through learning, which returns the relative phase to anti-phase. This is because the position of the support leg relative to the COM changes to reduce the difference. More specifically, the position of the support leg of the fast side moves forward relative to the COM, which decreases the

pitching moment by gravity, and the position of the support leg of the slow side moves backward, which increases the pitching moment (Fig. 4.14C), where we explain the reason why the positions of the support leg move relative to the COM due to the modification of the foot contact timing in the next paragraph. Because the vertical lines of the butterfly wings of the COP profile show the support position of the legs during the single support phase, these changes in the support position are verified from Fig. 4.12 for humans and from Fig. 4.13 for our model.

Next, we explain the reason why the positions of the support leg move relative to the COM due to the modification of the foot contact timing. Figure 4.15A and B show the temporal and spatial relationships, respectively, between the stance phase and single support phase durations of each leg for each configuration and stage of the speed condition. During the tied configuration, the timing and position of the center of the stance phase (white circles) are identical to those of the single support phase (black circles) in each leg. In the early stage of splitbelt configuration, the timing and position become different between their centers due to the changes in the relative phase between the legs and duty factors. More specifically, in the fast (slow) leg, the timing of the center of the single support phase becomes later (earlier) than that of the stance phase. Similarly, in the fast (slow) leg, the position of the center of the single support phase moves backward (forward) than that of the stance phase. During the late stage of splitbelt configuration, learning modulates the movement to reduce the difference between the predicted and actual foot contact timings. In the slow leg, because actual foot contact timing was earlier than the prediction at the early stage of splitbelt configuration, the predicted timing becomes earliear through learning, which increases the speed of the swing movement. As a result, actual foot contact timing at the late stage of splitbelt configuration becomes earlier than that in the early stage, as obserbed in humans [79, 111]. This reduces the difference in the timing between the centers of the stance phase and single support phase in each leg. This modulation of timing shows that in the fast (slow) leg, the position of the single support phase moves farward (backward) relative to that of the stance phase and that their center positions becomes identical again in each leg.

It is suggested that controlling the COM position contributes to improving locomotion

stability during the late adaptatioin of human splitbelt treadmill walking [69, 86, 111], which supports the adaptation mechanism mentioned above. However, note that adaptive behaviors of our robot were not characteristics that we specifically designed in the control model, but they emerged through the dynamic interactions between the robot mechanical system, spinal and cerebellar based locomotion control system, and environment.

4.4.2 Controlling global pattern through local information

In this study, sensory reflex and learning about foot contact timing of each leg resulted in appropriate modification of the interlimb coordination. This means that global pattern of walking (interlimb coordination) was manipulated through the modification of local information of each leg (foot contact timing). Because the left and right legs are connected through the trunk, the modification of the foot contact timing of one leg affects, and is affected by the other leg. Therefore, even if the modification is separately conducted in each leg, it influences the whole-body movement. In other words, without solving a high-order problem to determine the whole-body movement using the information of the whole body, solving a low-order problem using local information, such as foot contact timing of each leg, can produce appropriate whole-body movement through neuromechanical interactions. This idea is useful for control design of legged robots to produce adaptive locomotion using a small number of sensors.

4.4.3 Modification of spatiotemporal patterns of movement

Humans modulate spatiotemporal patterns of their movement to adapt to environmental changes. Walking on a splitbelt treadmill is a useful task to see the adaptation mechanism in the spatial and temporal patterns. In our model, we only focused on the temporal pattern, that is, foot contact timing for learning model. The temporal modification induced not only the changes in the temporal patterns of locomotion, such as the relative phase between the legs, but also the changes in the spatial pattern, such as the COP pattern. This means that the temporal modification of the robot movement induced the spatial modification through locomotion dynamics, as explained in Sec. 4.4.1. However,

from the measurement of humans, it is difficult to reveal which pattern is manipulated and induces the modificatoin of the other pattern. This modeling approach is useful to show a possibility of human gait strategy, which is difficult to clarify from the measurement.

4.4.4 Contributions of spinal cord and cerebellum to locomotor adaptation

In this study, we modeled a function of cerebellum to investigate the late adaptation in human splitbelt treadmill walking. The cerebellum contributes to coordinated movements through the prediction. For example, to move the arm during standing, humans modulate their posture before the arm movement to maintain the stability against the perturbation of COM due to the arm movement [26]. The cerebellum contributes to this anticipatory regulation. During locomotion, phase modulation responding to the stimulation to the nerves in the legs [25, 32, 43, 117] and reflexive reaction in the absence of sensory information of foot contact [56, 129] suggest that sensory information related to foot contact timing play an important role in modulating locomotor behavior. Especially in the splitbelt treadmill walking, soon after the splitbelt configuration starts, the vertical ground reaction forces at the foot contact timing (early stance phase) increased rapidly and then after a while they gradually reduced [86]. By contrast, at middle and late stance phases, they did not change during the splitbelt configuration. These observations suggest that the environmental change at the early stage of splitbelt configuration induced the difference between the predicted and actual foot contact timings and incraesed the ground reaction forces only in the early stance phase. Modification of the predicted timing to adapt to the environmental change reduced the ground reaction forces. We incorporated a learning model to regulate foot contact timing based on the error information between predicted and actual foot contact timings, which changed characteristic locomotion parameters, such as the relative phase between the legs, duty factors, and COP patterns, as observed in human splitbelt treadmill walking. Our modeling and results are consistent with observatios in humans and clarify the importance of modification of foot contact timing for adaptive locomotion from a dynamic viewpoint.

Adaptation in human splitbelt treadmill walking has two different time scales; early and late adaptations, which are mainly contributed by different layers in the neural system; spinal cord and cerebellum. The spinal cord produce motor commands through the RG and PF networks and modulates them immediately as a response of sensory input [50]. In fact, spinal cats walking on splitbelt treadmill showed rapid adaptive behavior like early adaptation [41, 42]. Our model without cerebellar learning model also showed rapid adaptive behavior like early adaptation due to our spinal CPG model [45]. The cerebellum receives efference copy from the spinal cord through the VSCT (ventral spinocerebellar tract) and sensory information through the DSCT (dorsal spinocerebellar tract) [10, 37]. Purkinje cells produce the output of the cerebellum to modulate motor commands based on the error information between the predicted sensory information from the efference copy and actual sensory information. This modification contributes to late adaptation, as suggested from the cerebellar damage that does not show late adaptation [88]. The reflexive response in the spinal cord and learning modulation in the cerebellum induce these two different time scales of adaptation. The reflexive response in the spinal cord secures to continue walking against environmental changes and under that condition, the cerebellum modulates the movements to walk more smoothly and effectively [39]. The two-layered model, which consists of the spinal CPG model with reflexive modulation of motor commands based on phase resetting and the cerebellar model with gradual modulation of the commands through learning, produced such two different time scales of adaptation.

4.4.5 Limitations of the approach and future work

In this study, we used a robotic platform to investigate human bipedal locomotion. The robot mechanical system is much simpler than musculoskeletal system of humans. In addition, the robot body is rigid and its joints are strictly controlled by motors, whereas humans are compliant because their joints are manipulated by muscles. Moreover, we used a much simpler locomotion control model than neural locomotion control system in humans. These difference caused quantitative differences in locomotion parameters, but our robot showed similar trends in adaptive behavior to that of humans in splitbelt

treadmill walking, as confirmed by the measurements of humans. This suggests that our simple robot mechanical and locomotion control systems capture the essential aspects to generate adaptive locomotor behavior as in humans.

As the cerebellar damage causes gait ataxia, the cerebellum has many functions for adaptive locomotion other than the interlimb and intralimb coordinations observed in splitbelt treadmill walking. For example, the cerebellum has a crucial role in dynamic regulation of balance to stabilize the walking behavior [89]. In addition, it contributes to motor control of voluntary and intentional leg movements, such as stepping over an obstacle [90]. To further clarify the cerebellar underlying mechanisms in walking, we intend to develop a more sophisticated model and a biologically plausible robot.

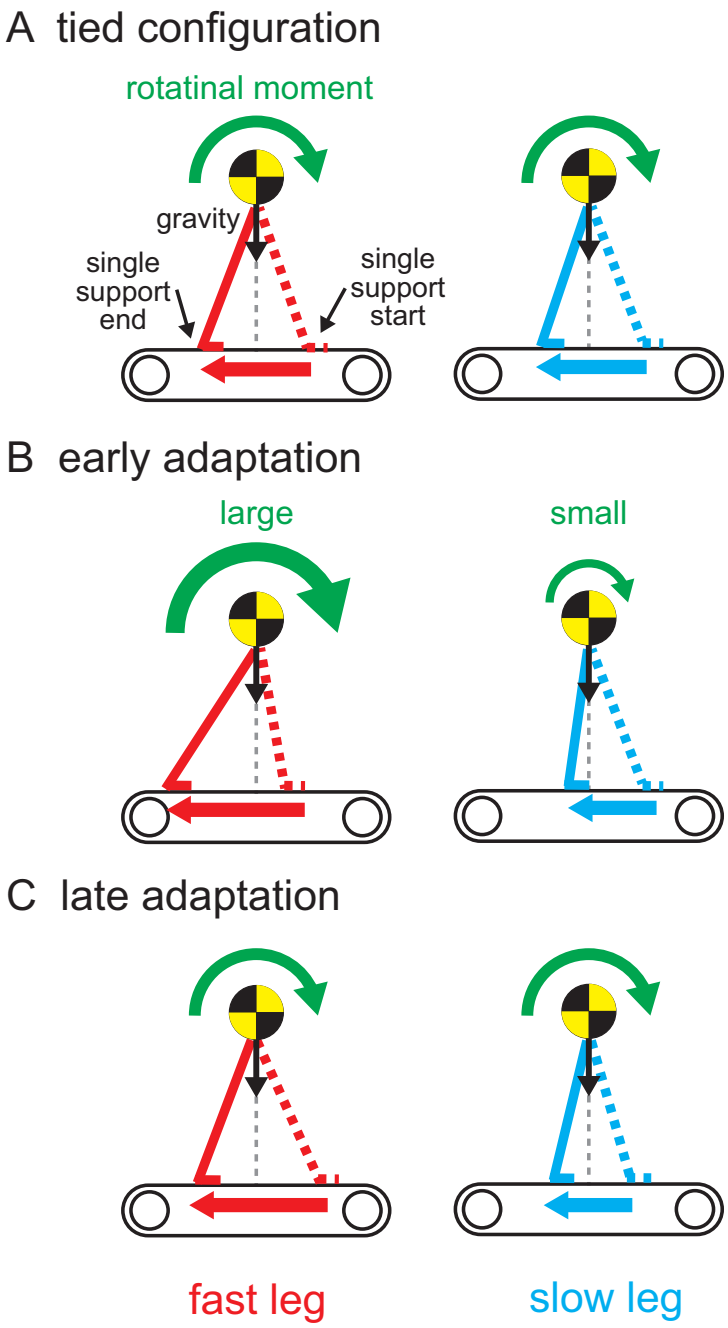

Fig. 4.14: Change of pitching moment due to change in belt speed. In (A) tied configuration, pitching moment is identical between legs. In (B) early stage of splitbelt configuration, increase of belt speed in fast side increases pitching moment during single support phase of fast leg, which induces early foot contact of contralateral (slow) leg. Similar mechanism is also applied to the other side and foot contact of fast leg is delayed. In (C) late stage of splitbelt configuration, difference of pitching moment between legs reduces by moving position of suppurt leg of fast side farward relative to COM and moving that of slow side backward.

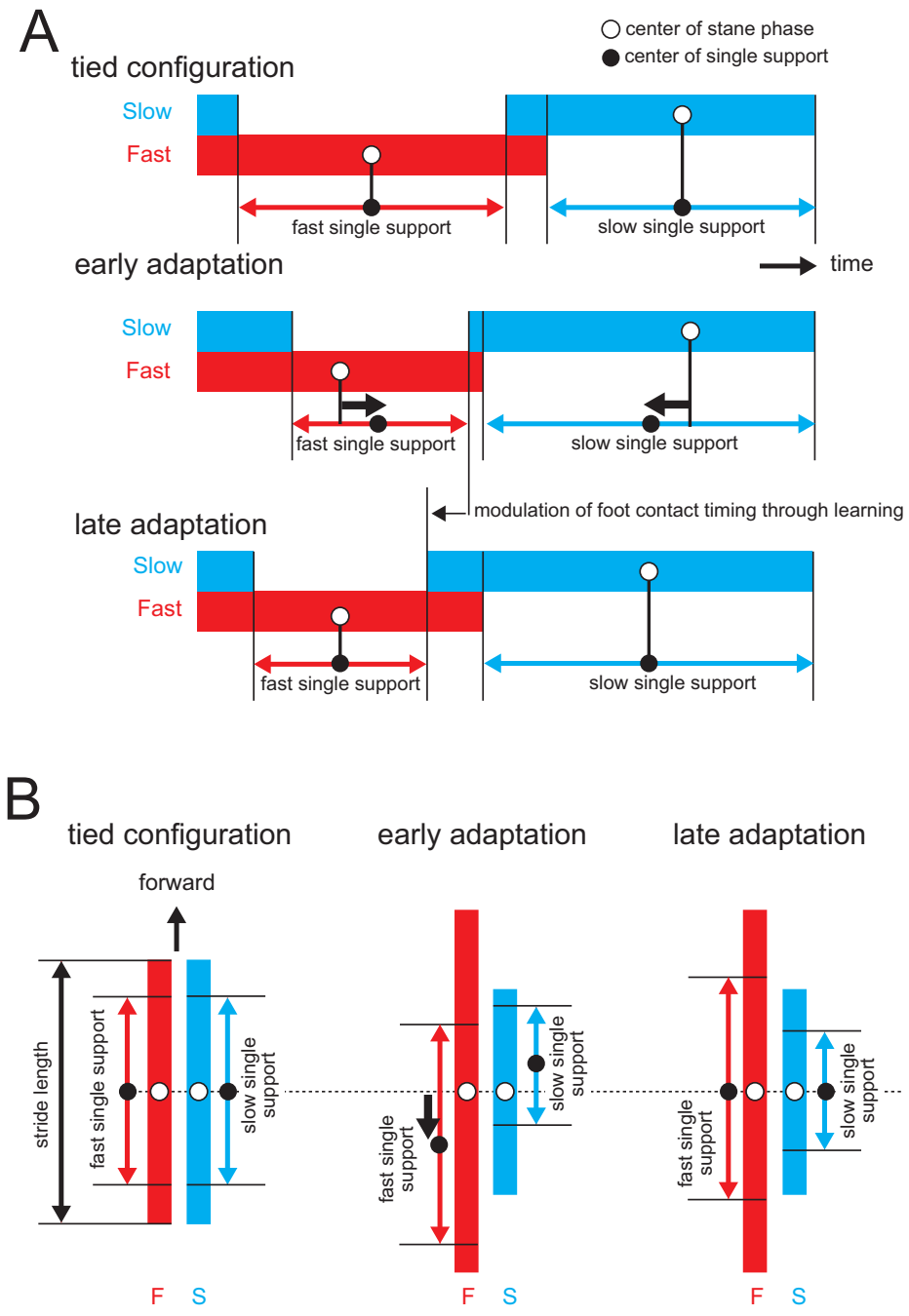

Fig. 4.15: Change in (A) temporal and (B) spatial relationships between stance and single support phases of each leg for each configuration and stage of the speed condition. White and black circles indicate center of stance and single support phases, respectively. In tied configuration, their center positions are identical in each leg. In early stage of splitbelt configuration, their center positions differ. In late stage of splitbelt configuration, their center positions become identical again.

Chapter 5

Conclusion

5.1 Summary

In this thesis, we investigated the adaptive locomotor behavior using robots and control model based on physiological findings. Especially, we focused on mechanism to generate interlimb coordination observed in biological system.

In Chapter 2, we focused on the gait generation and transition of a hexapod. Our model established the metachronal gait at slow locomotion speeds and the tripod gait at fast locomotion speeds, as observed in insect locomotion. Furthermore, it exhibited a metachronal-tripod gait transition with hysteresis. These results suggest that this model captured the essential aspects of the gait generation and transition (the most typical example of interlimb coordination) as in insect. A stability analysis using the return map clarified that the equilibrium points (gait pattern) change through the saddle-node bifurcation, which induces hysteresis in the gait transition. These results were because the stability structure changed through dynamic interactions among the body mechanical system, the nervous system, and the environment.

In Chapter 3, we investigated the interlimb coordination of a biped robot walking on a splitbelt treadmill using the locomotion control system developed in Chapter 2. Our robot established stable walking without changing the control strategy and parameters, despite a large discrepancy between the belt speeds. This was due to modulation of the locomotion rhythm and its phase through the phase resetting mechanism, which induces

the relative phase between leg movements to shift from antiphase, and caused the duty factors to be autonomously modulated depending on the speed discrepancy between the belts. In addition, the adaptive behavior showed qualitatively similar trend to early adaptation of the interlimb coordination in humans.

In Chapter 4, we investigated the splitbelt treadmill walking of biped model as in Chapter 3. In this chapter, we focused on the functional role of cerebellum. We developed a control model of cerebellum for walking based on physiological findings and incorporated it to the spinal CPG model used in Chapter 3. This model modified the motor commands produced by the spinal CPG model based on the error information between the predicted and actual foot contact timings through learning. We performed the robot and simulation experiments of a biped robot on a splitbelt treadmill and our results showed that characteristic locomotion parameters, such as the relative phase between the legs and duty factors, showed similar trend to early and late adaptations in human splitbelt treadmill walking. Our results suggested that the modulation of foot contact timing contributes to producing adaptive locomotion.

5.2 Future work

In this thesis, we used legged robot and control model based on physiological findings to understand the mechanism to generate adaptive locomotor behavior in humans and animals. However, there are many differences between the model and actual biological system. The robot mechanical system is much simpler than musculoskeletal system of humans and animals. In addition, the robot body is rigid and its joints are strictly controlled by motors, whereas humans and animals are compliant because their joints are manipulated by muscles. Moreover, we used a much simpler locomotion control model than neural locomotion control system in humans and animals. Despite these differences, our robots and control models produced adaptive locomotor behavior and these trends were qualitatively similar to those of humans and animals. This suggests our simple robot mechanical and locomotion control systems capture the essential aspects to generate adaptive locomotor behavior as in humans and animals. Therefore, in the

future, we should clarify what is essential and minimal element to generate adaptive locomotor behavior. These findings could be applied to control of legged robots.

Bibliography

[1] S. Aoi, Y. Egi, and K. Tsuchiya. Instability-based mechanism for body undulations in centipede locomotion. *Phys. Rev. E*, 87:012717, 2013.

[2] S. Aoi, Y. Egi, R. Sugimoto, T. Yamashita, S. Fujiki, and K. Tsuchiya. Functional roles of phase resetting in the gait transition of a biped robot from quadrupedal to bipedal locomotion. *IEEE Trans. Robot*, 28(6):1244–1259, 2012.

[3] S. Aoi, D. Katayama, S. Fujiki, N. Tomita, T. Funato, T. Yamashita, K. Senda, and K. Tsuchiya. A stability-based mechanism for hysteresis in the walk-trot transition in quadruped locomotion. *J. R. Soc. Interface*, 10(81):20120908, 2013.

[4] S. Aoi, T. Kondo, N. Hayashi, D. Yanagihara, S. Aoki, H. Yamaura, N. Ogihara, T. Funato, N. Tomita, K. Senda, and K. Tsuchiya. Contributions of phase resetting and interlimb coordination to the adaptive control of hindlimb obstacle avoidance during locomotion in rats: A simulation study. *Biol. Cybern.*, 107(2):201–216, 2013.

[5] S. Aoi, N. Ogihara, T. Funato, Y. Sugimoto, and K. Tsuchiya. Evaluating functional roles of phase resetting in generation of adaptive human bipedal walking with a physiologically based model of the spinal pattern generator. *Biol. Cybern.*, 102(5):37–387, 2010.

[6] S. Aoi, N. Ogihara, T. Funato, and K. Tsuchiya. Sensory regulation of stance-to-swing transition in generation of adaptive human walking: A simulation study. *Robot. and Auton. Syst.*, 60(5):685–691, 2012.

[7] S. Aoi and K. Tsuchiya. Locomotion control of a biped robot using nonlinear oscillators. *Auton. Robots*, 19(3):219–232, 2005.

[8] S. Aoi and K. Tsuchiya. Adaptive behavior in turning of an oscillator-driven biped robot. *Auton. Robots*, 23(1):37–57, 2007.

[9] S. Aoi, T. Yamashita, and K. Tsuchiya. Hysteresis in the gait transition of a quadruped investigated using simple body mechanical and oscillator network models. *Phys. Rev. E*, 83(6):061909, 2011.

[10] Y.I. Arshavsky, I.M. Gelfand, and G.N. Orlovsky. The cerebellum and control of rhythmical movements. *Trends Neurosci.*, 6:417–422, 1983.

[11] R. Alexander. Optimization and gaits in the locomotion of vertebrates. *Physiol. Rev.*, 69(4):1199–1227, 1989.

[12] U. Bässler, and A. Büschges. Pattern generation for stick insect walking movements? multisensory control of a locomotor program. *Brain Res. Rev.*, 27:65–88, 1998.

[13] A.J. Bastian. Learning to predict the future: the cerebellum adapts feedforward movement control. *Curr. Opin. Neurobio.*, 16:645–649, 2006.

[14] J. Bender, E. Simpson, B. Tietz, K. Daltorio, R. Quinn, and R. Ritzmann. Kinematic and behavioral evidence for a distinction between trotting and ambling gaits in the cockroach Blaberus discoidalis. *J. Exp. Biol.*, 214:2057–2064, 2011.

[15] G. Bosco and R.E. Poppele. Proprioception from a spinocerebellar perspective. *Physiol. Rev.*, 81:539–568, 2001.

[16] L.A. Boyd and C.J. Winstein. Cerebellar stroke impairs temporal but not spatial accuracy during implicit motor learning. *Neurorehabil. Neural Repair*, 18:134–143, 2004.

[17] D.J. Braun, J.E. Mitchell, and M. Goldfarb. Actuated dynamic walking in a seven-link biped robot. *Trans. Mech.*, 17(1):147–156, 2012.

[18] T.G. Brown. On the nature of the fundamental activity of the nervous centres: together with an analysis of the conditioning of rhythmic activity in progression,

and a theory of the evolution of function in the nervous system. *J. Physiol.*, 48:18–46, 1914.

[19] R.E. Burke, A.M. Degtyarenko, and E.S. Simon. Patterns of locomotor drive to motoneurons and last-order intemeurons: Clues to the structure of the CPG. *J. Neurophysiol.*, 86:447–462, 2001.

[20] A. Casabona, M. Valle, G. Bosco, A. Garifoli, S Lombardo, and V. Perciavalle. Anisotropic representation of forelimb position in the cerebellar cortex and nucleus interpositus of the rat. *Brain Res.*, 972:127–136, 2003.

[21] J.T. Choi and A.J. Bastian. Adaptation reveals independent control networks for human walking. *Nat. Neurosci.*, 10(8):1055–1062, 2007.

[22] A.H. Cohen, P.J. Holmes, and R.H. Rand. The nature of the coupling between segmental oscillators of the lamprey spinal generator for locomotion: A mathematical model. *J. Math. Biology*, 13:345–369, 1982.

[23] S.H. Collins, A.L. Ruina, R. Tedrake, and M. Wisse. Efficient bipedal robots based on passive-dynamicwalkers. *Science*, 307: 1082–1085, 2005.

[24] J. Collins and I. Stewart. Hexapodal gaits and coupled nonlinear oscillator models. *Biol. Cybern.*, 68:287–298, 1993.

[25] B.A. Conway, H. Hultborn, and O. Kiehn. Proprioceptive input resets central locomotor rhythm in the spinal cat. *Exp. Brain Res.*, 68:643–656, 1987.

[26] P.J. Cordo and L.M. Nashner. Properties of postural adjustments associated with rapid arm movements. *J. Neurophysiol.*, 47(2):287–302, 1982.

[27] H. Cruse, T. Kindermann, M. Schumm, J. Dean, and J. Schmitz. Walknet - a biologically inspired network to control six-legged walking. *Neural Networks*, 11:1435–1447, 1998.

[28] G. D'Angelo, Y. Thibaudier, A. Telonio, M.-F. Hurteau, V. Kuczynski, C. Dambreville, and A. Frigon. Modulation of phase durations, phase variations and temporal

coordination of the four limbs during quadrupedal split-belt locomotion in intact adult cats. *J. Neurophysiol.*, in press

[29] F. Delcomyn. The locomotion of the cockroach periplaneta americana. *J. Exp. Biol.*, 54:443–452, 1971.

[30] F. Delcomyn, and P.N.R. Usherwood. Motor activity during walking in the cockroach periplaneta americana. *J. Exp. Biol.*, 59:629–642, 1973.

[31] F.J. Diedrich and W.H. Warren. Why change gaits? Dynamics of the walk-run transition. *J. Exp. Psychol. Hum. Percept. Perform.*, 21:183–202, 1998.

[32] J. Duysens. Fluctuations in sensitivity to rhythm resetting effects during the eat's step cycle. *Brain Res.*, 133(1):190–195, 1977.

[33] J. Duysens, F. Clarac, and H. Cruse. Load-regulating mechanisms in gait and posture: Comparative aspects. *Physiol. Rev.*, 80:83–133, 2000.

[34] Ö. Ekeberg, M. Blümel, and A. Büschges. Dynamic simulation of insect walking. *Arthropod Struct. Dev.*, 33:287–300, 2004.

[35] G. Endo, J. Morimoto, T. Matsubara, J. Nakanishi, and G. Cheng. Learning CPG-based biped locomotion with a policy gradient method: application to a humanoid robot. *Int. J. Robot. Res.*, 27(2):213–228, 2008.

[36] C.T. Farley and C.R. Taylor. A mechanical trigger for the trot-gallop transition in horses. *Science*, 253:306–308, 1991.

[37] B. Fedirchuk, K. Stecina, K.K. Kristensen, M. Zhang, C.F. Meehan, D.J. Bennett, and H. Hultborn. Rhythmic activity of feline dorsal and ventral spinocerebellar tract neurons during fictive motor actions. *J. Neurophysiol.*, 109(2):375–388, 2013.

[38] J.P. Ferreira, M.M. Crisóstomo, and A.P. Coimbra. Adaptive PD controller modeled via support vector regression for a biped robot. *Trans. Contr. Syst. T.*, 21(3):941–949, 2013.

[39] J.M. Finley, A.J. Bastian, and J.S. Gottschall. Learning to be economical: the energy cost of walking tracks motor adaptation. *J. Physiol.*, 591(4):1081–1095, 2013.

[40] H. Forssberg and S. Grillner. The locomotion of the acute spinal cat injected with clonidine i.v.. *Brain Res.*, 50:184–186, 1973.

[41] H. Forssberg, S. Grillner, J. Halbertsma, and S. Rossignol. The locomotion of the low spinal cat. II. interlimb coordination. *Acta. Physiol. Scand.*, 108:283–295, 1980.

[42] A. Frigon, M.F. Hurteau, Y. Thibaudier, H. Leblond, A. Telonio, and G. D'Angelo. Split-belt walking alters the relationship between locomotor phases and cycle duration across speeds in intact and chronic spinalized adult cats. *J. Neurosci.* 33(19):8559–8566, 2013.

[43] A. Frigon, J. Sirois, and J.P. Gossard. Effects of ankle and hip muscle afferent inputs on rhythm generation during fictive locomotion. *J. Neurophysiol.*, 103(3):1591–1605, 2010.

[44] C. Fu, Y. Suzuki, K. Kiyono, P. Morasso, and T. Nomura. An intermittent control model of flexible human gait using a stable manifold of saddle-type unstable limit cycle dynamics. *J. R. Soc. Interface*, 11:20140958, 2014.

[45] S. Fujiki, S. Aoi, T. Yamashita, T. Funato, N. Tomita, K. Senda, and K. Tsuchiya. Adaptive splitbelt treadmill walking of a biped robot using nonlinear oscillators with phase resetting, *Auton. Robots.* 35(1):15–26, 2013.

[46] T. Funato, S. Aoi, H. Oshima, and K. Tsuchiya. Variant and invariant patterns embedded in human locomotion through whole body kinematic coordination. *Exp. Brain Res.*, 205(4): 497–511, 2010.

[47] D. Graham. Simulation of a model for the coordination of leg movement in free walking insects. *Biol. Cybern.*, 26(4):187–198, 1977.

[48] H. Geyer, A. Seyfarth, and R. Blickhan. Compliant leg behaviour explains basic dynamics of walking and running. *Proc. R. Soc. B*, 273:2861–2867, 2006.

[49] T.M. Griffin, R. Kram, S.J. Wickler and D.F. Hoyt. Biomechanical and energetic determinants of the walk-trot transition in horses. *J. Exp. Biol.*, 207:4215–4223, 2004.

[50] S. Grillner. Locomotion in vertebrates: central mechanisms and reflex interaction. *Physiol. Rev.*, 55(2):247–304, 1975.

[51] S. Grillner. The motor infrastructure: from ion channels to neuronal networks. *Nat. Rev. Neurosci.*, 4:573–586, 2003.

[52] R. Ghigliazza and P. Holmes. A minimal model of a central pattern generator and motoneurons for insect locomotion. *SIAM J. Appl. Dyn. Syst.*, 3(4):671–700, 2004.

[53] P.A. Guertin. The mammalian central pattern generator for locomotion. *Brain Res. Rev.*, 62:45–56, 2009.

[54] P. Guertin, M.J. Angel, M.-C. Perreault, and D.A. McCrea. Ankle extensor group I afferents excite extensors throughout the hindlimb during fictive locomotion in the cat. *J. Physiol.*, 487(1):197–209, 1995.

[55] N.C. Heglund and C.R. Taylor. Speed, stride frequency and energy cost per stride: how do they change with body size and gait?. *J. Exp. Biol.*, 138:301–318, 1998.

[56] G.W. Hiebert, M.A. Gorasssini, W. Jiang, A. Prochazka, and K.G. Pearson. Corrective responses to loss of ground support during walking. II. Comparison of intact and chronic spinal cats. *J. Neurophysiol.*, 71(2):611–622, 1994.

[57] M. Hoy and R. Zernicke. Modulation of limb dynamics in the swing phase of locomotion. *J. Biomech.*, 18:49–60, 1985.

[58] D.F. Hoyt and C.R. Taylor. Gait and energetics of locomotion in horses. *Nature*, 292(16):239–240, 1981.

[59] P. Holmes, R. Full, D. Koditschek, and J. Guckenheimer. The dynamics of legged locomotion: models, analyses, and challenges. *SIAM Rev.*, 48(2):207–304, 2006.

[60] A. Hreljac, R. Imamura, R.F. Escamilla, and W.B. Edwards. Effects of changing protocol, grade, and direction on the preferred gait transition speed during human locomotion. *Gait Posture*, 25:419–424, 2007.

[61] A. Ijspeert, A. Crespi, D. Ryczko, and J. Cabelguen. From swimming towalkingwith a salamander robot driven by a spinal cord model. *Science*, 315:1416–1420, 2007.

[62] A.J. Ijspeert. Central pattern generators for locomotion control in animals and robots: a review. *Neural Networks*, 21(4):642–653, 2008.

[63] A. Ishiguro, A. Fujii, and P.E. Hotz. Neuromodulated control of bipedal l ocomotion using a polymorphic CPG circuit. *Adaptive Behavior*, 11(1):7–18, 2003.

[64] M. Ito. Mechanisms of motor learning in the cerebellum. *Brain Res.*, 886:237–245, 2000.

[65] S. Ito, H. Yuasa, Z. Luo, M. Ito, and D. Yanagihara. A mathematical model of adaptive behavior in quadruped locomotion. *Biol. Cybern.*, 78:337–347, 1998.

[66] R.B. Ivry and S.W. Keele. Timing functions of the cerebellum. *J. Cogn. Neurosci.*, 1(2):136–152, 1989.

[67] R.B. Ivry, R.M. Spencer, H.N. Zelaznik, and J. Diedeichsen. The cerebellum and event timing. *Ann. N.Y. Acad. Sci.*, 978:302–317, 2012.

[68] E. Jankowska, A. Lundberg. Interneurons in the spinal cord. *Trends Neurosci.*, 4:230–233, 1981.

[69] K. Jansen, F. De Groote, J. Duysens, and I. Jonkers. Muscle contributions to center of mass acceleration adapt to asymmetric walking in healthy subjects. *Gait Posture*, 38:739–744, 2013.

[70] D. Jindrich and R. Full. Many-legged maneuverability: dynamics of turning in hexapods. *J. Exp. Biol.*, 202:1603–1623, 1999.

[71] M. Lafreniere-Roula and D.A. McCrea. Deletions of rhythmic motoneuron activity during fictive locomotion and scratch provide clues to the organization of the mammalian central pattern generator. *J. Neurophysiol.*, 94:1120–1132, 2005.

[72] S. Kimura, M. Yano, and H. Shimizu. A self-organizing model of walking patterns of insects. *Biol. Cybern.*, 69(3):183–193, 1993.

[73] H. Kimura, Y. Fukuoka, and A. Cohen. Adaptive dynamic walking of a quadruped robot on natural ground based on biological concepts. *Int. J. Robot. Res.*, 26(5):475–490, 2007.

[74] R. Kukillaya, J. Proctor, and P. Holmes. Neuromechanical models for insect locomotion: Stability, maneuverability, and proprioceptive feedback. *Chaos*, 19:026107, 2009.

[75] Y. Kuramoto. *Chemical oscillations, waves, and turbulences.* Springer-Verlag, Berlin, 1984.

[76] C.J.C. Lamoth, A. Daffertshofer, R. Huys, and P.J. Beek. Steady and transient coordination structures of walking and running. *Hum. Mov. Sci.*, 28:371–386, 2009.

[77] J.H. Lee, S. Okamoto, H. Koike, and K. Tani. Development and motion control of a biped walking robot based on passive walking theory. *Artif. Life Robotics*, 19:78–75, 2014.

[78] J. Li, and W. Chen. Energy-efficient gait generation for biped robot based on the passive inverted pendulum model. *Robotica*, 29:595–605, 2011.

[79] M.J. MacLellan, Y.P. Ivanenko, F. Massaad, S.M. Bruijn, J. Duysens, and F. Lacquaniti. Muscle activation patterns are bilaterally linked during split-belt treadmill walking in humans. *J. Neurophysiol.*, 111:1541–1552, 2014.

[80] P. Manoonpong, T. Geng, T. Kulvicius, B. Porr, and F. Wiirgiitter. Adaptive, fast walking in a biped robot under neuronal control and learning. *PLoS Comput. Biol.*, 3(7):e134, 2007.

[81] E. Marder and D. Bucher. Central pattern generators and the control of rhythmic movements. *Curr. Biol.*, 11:R986–R996, 2001.

[82] K. Matsuoka. Sustained oscillations generated by mutually inhibiting neurons with adaptation. *Bioi. Cybern.*, 52:367–376, 1985.

[83] K. Matsuoka. Mechanisms of frequency and pattern control in the neural rhythm generators. *Bioi. Cybern.*, 56:345–353, 1987.

[84] K. Matsukawa, H. Kamei, K. Monoda, and M. Udo. Interlimb coordination in cat locomotion investigated with perturbation. *Exp. Brain Res.*, 56:367–437, 1982.

[85] C. Maufroy, H.Kimura, and K. Takase. Integration of posture and rhythmicmotion controls in quadrupedal dynamicwalking using phase modulations based on leg loading/unloading. *Auton. Robots*, 28(3):331–353, 2010

[86] F. Mawase, T. Haizler, S. Bar-Haim, and A. Karniel. Kinetic adaptation during locomotion on a split-belt treadmill. *J. Neurophysiol.*, 109:2216–2227, 2013.

[87] D.A. McCrea and I.A. Rybak. Organization of mammalian locomotor rhythm and pattern generation. *Brain Res. Rev.*, 57:134–146, 2008.

[88] S.M. Morton and A.J. Bastian. Cerebellar contributions to locomotor adaptations during splitbelt treadmill walking. *J. Neurosci.*, 26(36):9107–9116, 2006.

[89] S.M. Morton and A.J. Bastian. Cerebellar control of balance and locomotion. *Neuroscientist*, 10:247–259, 2004.

[90] S.M. Morton, G.S. Dordevic, and A.J. Bastian. Cerebellar damage produces contextdependent deficits in control of leg dynamics during obstacle avoidance. *Exp. Brain Res.*, 156(2):149–163, 2004.

[91] M. Nakanishi, T. Nomura, and S. Sato. Stumbling with optimal phase reset during gait can prevent a humanoid from falling. *Bioi. Cybern.*, 95:503–515, 2006.

[92] J. Nakanishi, J. Morimoto, G. Endo, G. Cheng, S. Schaal, and M. Kawato. Learning from demonstration and adaptation of biped locomotion. *Robot. Auton. Syst.*, 47(2-3):79–91, 2004.

[93] J. Nishii. An analytical estimation of the energy cost for legged locomotion. *J. Theor. Biol.*, 238:636–645, 2006.

[94] P.D. Nixon and R.E. Passingham. Predicting sensory events. The role of the cerebellum in motor learning. *Exp. Brain Res.*, 138:251–257, 2001.

[95] T. Nomura, K. Kawa, Y. Suzuki, M. Nakanishi, and T. Yamasaki. Dynamic stability and phase resetting during biped gait. *Chaos*, 19:026103, 2009.

[96] K. Ohgane and K.I. Ueda. Instability-induced hierarchy in bipedal locomotion. *Phys. Rev. E*, 77:051915, 2008.

[97] K. Ohgane and K.I. Ueda. Stabilizing bipedal walking on posts through multiple constraints. *Phys. Rev. E*, 81:041909, 2010.

[98] J.X. O'Reilly, M.M. Mesulam, and A. C. Nobre. The cerebellum predicts the timing of perceptual eventse. *J. Neurosci.*, 28(9):2252–2260, 2008.

[99] G.N. Orlovsky, T. Deliagina, and S. Grillner. *Neuronal control of locomotion: from mollusc to man*. Oxford University Press, 1999.

[100] Y. Otoda, H. Kimura, and K. Takase. Construction of a gait adaptation model in human split-belt treadmill walking using a two-dimensional biped robot. *Adv. Robot.*, 23(5):535–561, 2009.

[101] D. Owaki, T. Kano, K. Nagasawa, A. Tero, and A. Ishiguro. Simple robot suggests physical interlimb communication is essential for quadruped walking. *J. R. Soc. Interface*, 10:20120669, 2013.

[102] K. Pearson. The control of walking. *Sci. Am.*, 235(6):72–86, 1976.

[103] K. Pearson, Ö. Ekeberg, and A. Büschges. Assessing sensory function in locomotor systems using neuro-mechanical simulations. *Trends Neurosci.* 29(11):625–631, 2006.

[104] R. Pfeifer, M. Lungarella, and F. Iida. Self-organization, embodiment, and biologically inspired robotics. *Science*, 318:1088–1093, 2007.

[105] R.E. Poppele and G. Bosco. Sophisticated spinal contributions to motor control. *Trends Neurosci.*, 26:269–276, 2003.

[106] R.E. Poppele, G. Bosco, and A.M. Rankin. Independent representations of limb axis length and orientation in spinocerebellar response components. *J. Neurophysiol.*, 87:409–422, 2002.

[107] J. Proctor, R. Kukillaya, and P. Holmes. A phase-reduced neuro-mechanical model for insect locomotion: feed-forward stability and proprioceptive feedback. *Phil. Trans. R. Soc. A*, 368:5087–5104, 2010.

[108] T. Prokop, W. Berger, W. Zijlstra, and V. Dietz. Adaptational and learning processes during human split-belt locomotion: interaction between central mechanisms and afferent input. *Exp. Brain Res.*, 106:449–456, 1995.

[109] A.J. Raynor, C.J. Yi, B. Abernethy, and Q.J. Jong. Are transitions in human gait determined by mechanical, kinetic or energetic factors?. *Hum. Mov. Sci.*, 21:785–805, 2002.

[110] J.L. Raymond, S.G. Lisberger, and M.D. Mauk. The cerebellum: a neuronal learning machine?. *Science*, 272(5265):1126–1131, 1996.

[111] D.S. Reisman, H.J. Block, and A.J. Bastian. Interlimb coordination during locomotion: What can be adapted and stored?. *J. Neurophysiol.*, 94:2403–2415, 2005.

[112] R.E. Ritzmann, R.D. Quinn, and M.S. Fischer. Convergent evolution and locomotion through complex terrain by insects, vertebrates and robots. *Arthropod Struct. Dev.*, 33:361–379, 2004.

[113] LA. Rybak, N.A. Shevtsova, M. Lafreniere-Roula, and D.A. McCrea. Modelling spinal circuitry involved in locomotor pattern generation: insights from deletions during fictive locomotion. *J. Physiol.*, 577(2):617–639, 2006.

[114] I.A. Rybak, K. Stecina, N.A. Shevtsova, and D.A. McCrea. Modelling spinal circuitry involved in locomotor pattern generation: insights from the effects of afferent stimulation. *J. Physiol.*, 577(2):641–658, 2006.

[115] A. Sarkar, and A. Dutta. 8-DoF biped robot with compliant-links. *Robot. Auton. Syst.*, in press.

[116] T. Sato, S. Sakaino, E. Ohashi, and K. Ohnishi. Walking trajectory planning on stairs using virtual slope for biped robots. *IEEE Trans. Ind. Electron.*, 58(4):1385–1396, 2011.

[117] E.D. Schomburg, N. Petersen, I. Barajon, and H. Hultborn. Flexor reflex afferents reset the step cycle during fictive locomotion in the cat. *Exp. Brain Res.*, 122(3):339–350, 1998.

[118] V. Segers, P. Aerts, M. Lenoir, and D. De Clercq. Spatiotemporal characteristics of the walk-to-run and run-to-walk transition when gradually changing speed. *Gait Posture*, 29:227–254, 2006.

[119] M.L. Shik and G.N. Orlovsky. Neurophysiology of locomotor automatism. *Phsyiol. Rev.*, 56(3):465–501, 1976.

[120] R.M. Spencer, R.B. Ivry, and H.N. Zelaznik. Role of the cerebellum in movements: control of timing or movement transitions?. *Exp. Brain Res.*, 161(3):383–396, 2005.

[121] C.P. Spirito, and D.L. Mushrush. Interlimb coordination during slow walking in the cockroach I. effects of substrate alterations. *J. Exp. Biol.*, 78:233–243, 1979.

[122] M. Srinivasan and A. Ruina. Computer optimization of a minimal biped model discovers walking and running. *Nature*, 439:72–75, 2006.

[123] S. Steingrube, M. Timme, F. Worgotter, and P. Manoonpong. Self-organized adaptation of a simple neural circuit enables complex robot behaviour. *Nature Physics*, 6:224–230, 2010.

[124] P.A. Stevenson and W. Kutsch. A reconsideration of the central pattern generator concept for locust flight. *J. Comp. Physiol. A*, 161:115–129, 1987.

[125] G. Taga, Y. Yamaguehi, and H. Shimizu. Self-organized control of bipedal locomotion by neural oscillators in unpredictable environment. *Biol. Cybern.*, 65:147–159, 1991.

[126] T. Tang and D. Macmillan. The effects of sensory manipulation upon interlimb coordination during fast walking in the cockroach. *J. Exp. Biol.*, 125:107–117, 1986.

[127] T. Tóth, S. Knops, and S. Daun-Gruhn. A neuromechanical model explaining forward and backward stepping in the stick insect. *J. Neurophysiol.*, 107(12):3267–3280, 2012.

[128] M.T. Turvey, K.G. Holt, M.E. LaFlandra, and S.T. Fonseca. Can the transition to and from running and the metabolic cost of running be determined from the kinetic energy of running?. *J. Mot. Behav.*, 31:265–278, 1999.

[129] M.H. van der Linden, D.S. Marigold, F.J. Gabreels, and J. Duysens. Muscle reflexes and synergies triggered by an unexpected support surface height during walking. *J. N europhysiol.*, 97(5):3639–3650, 2007.

[130] T. Wadden and Ö. Ekeberg. A neuro-mechanical model of legged locomotion: single leg control. *Biol. Cybern.*, 79(2):161–173. 1998.

[131] S. Wickler, D. Hoyt, E. Cogger, and G. Myers. The energetics of the trot-gallop transition. *J. Exp. Biol.*, 206:1557–1564, 2003.

[132] D.M. Wilson. Insect walking. *Annu. Rev. Entomol.*, 11:103–122, 1966.

[133] D.M. Wolpert, R.C. Miall, and M. Kawato. Internal models in the cerebellum. *Trends Cogn. Sci.*, 2(9):338–347, 1998.

[134] S. Yakovenko, V. Gritsenko, and A. Prochazka. Contribution of stretch reflexes to locomotor control: A modeling study. *Biol. Cybern.*, 90:146–155, 2004.

[135] D. Yanagihara and I. Kondo. Nitric oxide plays a key role in adaptive control of locomotion in cat. *Proc. Nat. Acad. Sci. USA*, 93:13292–13297, 1996.

[136] D. Yanagihara, M. Udo, I. Kondo, and T. Yoshida. A new learning paradigm: adaptive changes in interlimb coordination during perturbed locomotion in decerebrate cats. *Neurosci. Res.*, 18:241–244, 1993.

[137] T. Yamasaki, T. Nomura, and S. Sato. Possible functional roles of phase resetting during walking. *Biol. Cybern.*, 88:468–496, 2003.

[138] T. Yamasaki, T. Nomura, and S. Sato. Phase reset and dynamic stability during human gait. *BioSystems*, 71:221–232, 2003.

Published paper

- S. Fujiki, S. Aoi, T. Yamashita, T. Funato, N. Tomita, K. Senda, and K. Tsuchiya, Adaptive splitbelt treadmill walking of a biped robot using nonlinear oscillators with phase resetting, *Autonomous Robots*, 35(1):15–26, 2013.

- S. Fujiki, S. Aoi, T. Funato, N. Tomita, K. Senda, and K. Tsuchiya, Hysteresis in the metachronal-tripod gait transition of insects: A modeling study, *Physical Review E*, 88:012717, 2013.

- S. Fujiki, S. Aoi, T. Funato, N. Tomita, K. Senda, and K. Tsuchiya, Learning of foot-contact timing of each leg induces the late adaptation of interlimb coordination in human split-belt treadmill walking: a robotics study, *Journal of the royal society interface*. (submitted)